Sodium-Fluoride clusters:

A theoretical study

A Thesis Presented

by

Christian Gerhard Schmidt

to

The Graduate School

in Partial Fulfillment of the

Requirements

for the Degree of

Master of Arts

In

Physics

Stony Brook University

August 2004

Stony Brook University

The Graduate School

Christian Gerhard Schmidt

We, the thesis committee for the above candidate for the

Master of Arts degree,

hereby recommend acceptance of this thesis.

_____

Dr. Philip B. Allen
Advisor
Professor of Physics, Department of Physics and Astronomy

_____

Dr. Thomas C. Weihnacht
Chairman
Professor of Physics, Department of Physics and Astronomy

_____

Dr. David O. Welch
Outside member
Senior Materials Scientist, Materials Science Department
Brookhaven National Laboratory

This thesis is accepted by the Graduate School.

_____

Dean of the Graduate School

Abstract of the Thesis

Sodium-Fluoride clusters:

A theoretical study

by

Christian Gerhard Schmidt

Master of Arts

in

Physics

Stony Brook University

2004

Using density functional theory, geometries, energies and dipoles are calculated for a range of Sodium-Fluoride clusters. Starting with the free ions and atoms, the size dependence of these properties is studied up to the largest investigated cluster, $Na_{18}F_{18}$. In addition, the vibrational spectra with the infrared- and Raman-activities of the modes are computed. Electronic and vibrational polarizabilities are also calculated, where we used the dependence of the vibrational part on the vibrational frequencies and the dynamical charges of the cluster. Compared to the sum of the ionic values, an increase in the electronic polarizability is found, which is especially pronounced for small clusters. This phenomenon is explained with a LCAO model for the HOMO and LUMO orbitals of those clusters. In general, a strong dependence of all cluster parameters on the

conformation of the constituting atoms can be found. Therefore the application of classical models is restricted to specific cases, where they can be highly useful guidelines, as is shown in the example of the quadrupole polarizability of the Na_4F_4 cube cluster.

Table of Contents

List of Figures

List of Tables

Chapter 1

Density functional theory

1.1 Introduction & Theory

In the following thesis, we study a broad range of NaF-clusters with density functional theory (explained in the present chapter). Starting with the single nuclei cases and going to clusters as large as $Na_{18}F_{18}$, properties like geometry, energies, dipole moments and polarizabilities, as well as the vibrational spectra and their infrared and Raman activity are computed in chapter 2. Several interesting and surprising results are found, e.g. a large increase of the electronic polarizability in smaller clusters compared to the sum of the free ion values. Most of the phenomena are investigated and interpreted quantum mechanically.

Furthermore, we look at the formation energy of several clusters to estimate this number for the bulk crystal. Vibrational modes and their geometrical shapes are computed for many clusters by using group theory. Their dependence on the cluster geometry becomes especially obvious for the two isomers of Na_4F_4 (cube and ring).

Following this, chapter 3 contains a summary of classical models. In addition, two specific cases are analysed classically with respect to induced dipoles & quadrupoles as well as polarizabilities.

1.1.1 A brief history

With the development of quantum mechanics at the beginning of the previous century, the knowledge of physics was enriched by a powerful theory, whose capability cannot be underestimated. Nevertheless it was evident that apart from the very simplest problems it is almost always impossible to find good approximate solutions to Schroedinger's

equation, the task becoming more and more intricate with the number of particles in the system.

For many-particle systems Hartree and Fock developed an iterative method and finally in the 1960's Kohn, Hohenberg and Sham presented their first formulation of a method which only tries to find the total electron ground state density instead of the whole many-particle wavefunction [1,2], which was later named density functional theory (DFT). The heart of DFT is that the problem of solving Schroedinger's many-particle equation can be reduced to a set of effective single-particle equations, where the only non-straightforward part is a functional of the density which models the exchange and correlation part of the total energy (E_{xc}). The first practical functional was the local-density-approximation (LDA), but many different models have been and are still developed, among them the by now standard generalized-gradient-approximations (GGA).

Currently DFT is a highly useful tool to tackle a large number of problems and the major remaining task is still the improvement of the E_{xc}-functional. The interested reader can find a more detailed discussion of the content of subchapter 1.1 in [3].

1.1.2 The most important ideas behind DFT

Before we work out the theoretical framework and finally arrive at the desired Kohn-Sham-equations, which then have to be iterated until self-consistency is reached, it should be helpful to summarize the general ideas that lead to DFT.

Knowing that for chemistry and solid state physics we only need to think about electromagnetic interactions in the framework of quantum mechanics, it is important to conceive procedures that simplify this task. The first principle applied in DFT is the Born-Oppenheimer approximation, which means that we essentially treat the nuclei classically and only consider the electrons moving in their electrostatic potential. As a second step we agree that the multi-electron wavefunction contains far more information than we need, and therefore merely look for the electron density. Last but not least we learn from the Ritz variational principle, that the ground state of a system always gives the global minimum of the expectation value of the Hamiltonian and we will use this and only look for the total ground state energy and charge density.

As a final remark it must be mentioned that this approach will not be unique, but that there will still remain one contribution to the total energy that can not be expressed in known quantities. Instead, this energy term which models the exchange and correlation energy of the electrons has to be approximated by educated guessing (see 1.1.1).

1.1.3 Defining density functionals

In order to set up the equations which are to be solved to get the total ground state electron density n(**r**) and energy E, we have to make some definitions. First, a functional F[f] is mathematically defined as a rule which assigns a numerical value to an input function, where F is the functional and f the input function.

Next we define the functional derivative δF/δn(**r**), here already as an example with n(**r**) as input:

$$\delta F = \int d^3 r \left(\frac{\delta F}{\delta n(r)} \right) \delta n(r) \tag{1.1}$$

Using these definitions the problem of a many-body Hamiltonian for electrons in an external potential can now be rewritten (where we omit the spin for convenience), using atomic units.

$$\hat{H} = -\frac{1}{2} \sum_{i=1}^{N} \nabla_i^2 + \sum_{i=1}^{N} v(r_i) + \frac{1}{2} \sum_{i \neq j} \frac{1}{|r_i - r_j|} = \hat{T} + \hat{V}_{ext} + \hat{V}_{ee} \tag{1.2}$$

By setting up this N-electron Hamiltonian we implicitly used the Born-Oppenheimer approximation, therefore the nuclei contribute only as a source of $\hat{V}_{ext}$ and the last contribution results from the self-interaction of the electrons.

The ground state of $\hat{H}$ is then given by the minimization of its expectation value,

$$E = \min_{\Psi} \left\langle \Psi \left| \hat{H} \right| \Psi \right\rangle \tag{1.3}$$

where Ψ is the many-particle wavefunction.

Now it is useful to define the functional F[n]

$$F[n] = \min_{|\Psi|^2 = n} \left\langle \Psi \left| \hat{T} + \hat{V}_{ee} \right| \Psi \right\rangle = \left\langle \Psi_n^{min} \left| \hat{T} + \hat{V}_{ee} \right| \Psi_n^{min} \right\rangle \tag{1.4}$$

where the minimization is over all Ψ that result in the given density n. Realizing that the expectation value of the external potential depends only on n, but not on Ψ, we get:

$$E = \min_n E_v[n] = \min_n \left(F[n] + \int d^3 r \, v(r) n(r) \right) \tag{1.5}$$

The density we get from this minimization process is the desired ground state density and it can also be proven that there exist unambiguous pairs of $\hat{V}_{ext}$ and n(**r**). That means that for each n(**r**) there exists one unique $\hat{V}_{ext}$ and vice versa [1]. The only other existing constraint is a fixed number of particles, which means:

$$\int d^3 r \, n(r) = N \tag{1.6}$$

To split F[n] further up, we first find the wavefunction which minimizes the expectation value of $\hat{T}$, by using the functional $T_s[n]$,

$$T_s[n] = \min_{|\Psi|^2 = n} \left\langle \Psi \left| \hat{T} \right| \Psi \right\rangle = \left\langle \Phi_n^{\min} \left| \hat{T} \right| \Phi_n^{\min} \right\rangle \tag{1.7}$$

and introduce a functional U[n] which represents the classical electrostatic self-interaction energy of the charge density :

$$U[n] = \frac{1}{2} \int d^3 r \int d^3 r' \frac{n(r)n(r')}{|r - r'|} \tag{1.8}$$

For a given charge density, $\left\langle \hat{V}_{ext} \right\rangle$, $T_s[n]$ and U[n] can be evaluated without making any additional assumptions, but in order to get the correct energy we have to add a functional which contains all the contributions we omitted in those three terms $\Rightarrow E_{xc}[n]$.
Formally, $E_{xc}[n]$ can be defined in the following way :

$$E_{xc}[n] = F[n] - U[n] - T_s[n] \tag{1.9}$$

Furthermore we now look at the exchange and correlation parts separately:

$$E_x[n] = \left\langle \Phi_n^{\min} \left| \hat{V}_{ee} \right| \Phi_n^{\min} \right\rangle - U[n] \tag{1.10}$$

$$E_c[n] = \left\langle \Psi_n^{\min} \left| \hat{T} + \hat{V}_{ee} \right| \Psi_n^{\min} \right\rangle - \left\langle \Phi_n^{\min} \left| \hat{T} + \hat{V}_{ee} \right| \Phi_n^{\min} \right\rangle \tag{1.11}$$

It is obvious, that $E_c \leq 0$, because the first part of it actually minimizes the expectation value. In Hartree-Fock theory (HF) the exchange energy is treated exactly, whereas correlation is omitted, i.e. the HF total energy only represents an upper bound.

As already mentioned in the previous section, the major difficulty in DFT is to find a functional, which models $E_{xc}[n]$ as well as possible. The most basic approach is to calculate E_{xc} per unit density for a homogeneous electron gas (LDA), which can be done analytically for the exchange and well approximated for the correlation, and then simply express $E_{xc}[n]$ as:

$$E_{xc}[n] = \int d^3 r \, e_{xc}(n(r)) \tag{1.12}$$

where $e_{xc}(n)$ is the energy density of the homogeneous electron gas with constant electron density n. All those facts imply that this approximation is especially good for slowly varying densities. As a next step in refining this functional one normally introduces a functional that not only depends on n, but also on ∇n. All functionals of this type are labelled GGA, as already mentioned. They are currently used in most applications, because they find a good balance between computer time and accuracy.

1.1.4 The Kohn-Sham equations

After we have shown how to formally reduce the problem to a minimization in n(**r**), it is time to take the final step and derive the equations we use to perform this process.

We start by imagining n(**r**) made up of N singly occupied orbitals:

$$n(r) = \sum_{k=1}^{N} \left| \psi_k(r) \right|^2 \tag{1.13}$$

Next, the fact is used that the variational principle can be applied to the total energy functional after we used the method of Lagrange multipliers, i.e.:

$$\frac{\delta}{\delta \psi_i^*} \left\{ E[n] - \sum_{k=1}^{N} \varepsilon_k \int \left| \psi_k(r) \right|^2 \right\} \tag{1.14}$$

$$\text{with} \quad E[n] = T_s[n] + U[n] + \int d^3r \, v(r) n(r) + E_{xc}[n] \tag{1.15}$$

For the different *i*, this leads to a set of effective single particle equations, the so-called Kohn-Sham equations:

$$\left\{ -\frac{\nabla^2}{2} + \int d^3r' \frac{n(r')}{|r - r'|} + v(r) + \frac{\delta E_{xc}}{\delta n(r)} \right\} \psi_i(r) = \varepsilon_i \psi_i(r) \tag{1.16}$$

The four contributing terms in the operator on the left-hand side of (1.16) are just the functional derivatives of the corresponding functionals in (1.15). These equations together with (1.13) are all that is needed for getting the desired results. They simply have to be iterated until self-consistency is reached. However, a few remarks are necessary to explain the use and implementation of these equations.

Strictly speaking it is not allowed to give physical meaning to the functions Ψ_i and the Kohn-Sham energy eigenvalues ε_i. Only the total electron density has a counterpart in reality. Furthermore, the total energy of the system is not the sum of the ε_i, but (1.15), which (using the ε_i) can be rewritten as:

$$E[n] = \sum_{k=1}^{N} \varepsilon_k - \frac{1}{2} \int d^3r \, d^3r' \frac{n(r)\,n(r')}{|r-r'|} + E_{xc}[n] - \int d^3r \frac{\delta E_{xc}}{\delta n(r)} n(r) \qquad (1.17)$$

In addition to that we have the energy contributions from the nuclear repulsion, which are essential if we want to calculate the vibrational frequencies of a system. Furthermore, it can be seen that we can calculate an infinite number of eigenfunctions, but it should be clear that only the N lowest lying ones are occupied. In fact, only those are used as new input for the next iteration. This means that if we would occupy one of the energetically higher levels instead of one which is normally occupied after self-consistency is reached, the equations would become inconsistent again. After that, we would again get the same ground state after some iterations. A closing remark is also due here regarding the iteration process. Often instabilities will be found if we use only the new Ψ_i as input for n(**r**). Instead in most practical applications a linear combination of the previous few results is used.

1.2   The NRLmol computer code

Having discussed the ideas and procedures that are applied in DFT in general, the next section presents the implementation of DFT used in this work: The NRLmol computer code. It was developed by M. Pederson *et al.* [4-10] and is freely available for non-profit use. The present subchapter 1.2 will mainly be a summary of references [4,5,8] and gives an overview of the properties and structure of NRLmol.

1.2.1   Characteristics and features

Since NRLmol is completely based on DFT, the basic processes involved have already been explained in 1.1. Nevertheless, there still is some variety among the different implementations that are currently used in the DFT-community. For example it has to be decided whether all electrons should be included in the formalism or whether pseudopotentials are to be used and only the outer electrons of each atom are treated with DFT. In NRLmol all-electron computations are the default and have consistently been used throughout this work, but there also exists the possibility to use pseudopotentials.

Other important features are the full exploitation of the symmetry point group of the molecule and the use of a special integration mesh. Both features contribute to lowering

the computation cost and we will discuss the method of finding an appropriate integration mesh in 1.2.2. Furthermore the electronic Kohn-Sham orbitals are expanded in a Gaussian basis set and the whole system is accommodated in a 3-dimensional box. This box is divided by the integration mesh and is large enough that the electron density outside the box is zero.

All the previously mentioned facts now describe the process of finding the energetically most favourable electron density for a given set of nuclear coordinates. To complete the process, we also have to find the ground state configuration of the nuclei. For this purpose NRLmol not only computes the total energy for a certain configuration, but also the forces on all nuclei, by making total derivatives of the total energy. These are made up of the "classical" Hellmann-Feynman forces (1.18) plus the Pulay correction which includes all the quantum terms.

$$\vec{F}_{HF}(\nu) = Z_\nu \sum_\mu Z_\mu \frac{\vec{R}_\nu - \vec{R}_\mu}{\left|\vec{R}_\nu - \vec{R}_\mu\right|^3} + Z_\nu \int d^3 r\, n(\vec{r}) \frac{\vec{r} - \vec{R}_\nu}{\left|\vec{r} - \vec{R}_\nu\right|^3} \tag{1.18}$$

With this information a new guess for the nuclear coordinates is made, until the forces fulfill the given convergence criterion.

Using this program, we can calculate the ground-state geometry, the total energy as well as the single Kohn-Sham energy levels and the electronic densities. In addition spins can be included and LDA as well as GGA exchange-correlation functionals can be chosen. After having iterated until the ionic forces are converged, the additional program 'specsym' can be used to calculate the vibrational frequencies, intensities and Raman or infrared (IR) activities, as well as the electronic and vibrational polarizability tensor (see 1.2.3).

1.2.2 The variational mesh

The main computational effort reduces to the integration of functions in the box. Since fast Fourier transforms are unacceptably slow in finite systems, the integration has to be done by dividing the box into points and volume elements, where the functions are evaluated. The standard procedure is to choose a subset of a complete set of basis functions and find points and volume elements, so that the integrals over those functions are reproduced exactly. On the other hand, NLRmol uses meshes that are more computationally demanding to set up, but improve the accuracy considerably. Therefore the effort of setting up the mesh pays off (~equal to one full electron density optimization for given nuclear positions), since later on a large number of iterations will be needed until the nuclear positions are converged and computer time is saved during each of them.

As first step to set up the mesh, space is divided into three different types of regions: atomic spheres, interstitial parallelepipeds and excluded cube regions (for details see [4]). For each of these regions slightly different techniques are applied, but the most important part is the introduction of a continuous transformation of one-dimensional Gaussian quadrature (GQ) meshes. These transformed meshes can be varied continuously, to reproduce a wide range of test integrals accurately. By using them, one gets an exponential dependence of the accuracy on the number of mesh points, which implies that extremely high accuracy is possible, in principle arbitrarily accurate. In addition, fewer mesh points are required to reach the same level of accuracy (factor of 2 compared to normal GQ meshes and 10 for plane-wave meshes). This results in savings of computer time during the iterations.

1.2.3 Vibrations and Polarizabilities

With the forces on the ions converged to zero, the additional program 'specsym' can be used to make calculations on the vibrational frequencies, their intensities and activities, as well as the polarizabilities. These properties are computed by performing a set of calculations where the ground state configuration is either disturbed by an applied electric field, or one of the nuclear coordinates is a little bit displaced. This process is greatly simplified by making use of the point group symmetries of the cluster.

It is important to mention that this enterprise is not affected by electron tunnelling due to the constant electric field. This can be understood in the following way: Since we work in a box, there is no difference between an applied field of great wavelength and the constant field. In experiments, tunnelling is normally also not observed because the observation times are shorter than the time required for electrons to decay to infinity by tunnelling.

Although getting the frequencies of the vibrational modes and the electronic polarizability is rather basic, the intensities are more delicate. Especially intensities of the Raman-active vibrations are hard, since they depend on a third-order derivative of the total energy, whereas those of the infrared (IR) modes only depend on a second order one. Therefore the agreement with experiment is in general better for the IR modes, but it is essential to use GGA functionals, since the error becomes substantially higher for LDA functionals. Summarizing, the standard deviations can approximately be estimated to be about 50%, strongly depending on basis set size. This estimate is of course not very exact, but can at least give a basic feeling for the quality of the results.

In the newest version of 'specsym' (written recently by M. Pederson motivated by observations made during this research), the output also contains the vibrational part of the polarizability, which is computed by using the dynamical charges and the vibrational

frequencies of the molecule. For the diatomic molecule this formula is discussed in detail in 2.3.1., and the general formula is given by (2.58).

1.3 Motivation and thesis goals

Since all we discussed so far was DFT and its implementation, it is already clear what the main content of this thesis will be. However, when this project was started, the intentions were rather going the other way round: Having a short chapter on NRLmol calculations, including a discussion of the results, then moving on to working out a classical model, fitted to the NRLmol results, and a rather thorough study of small NaF clusters. The motivation was that classical models do fairly well on crystal structures and that a simple model, which at least modestly accurate accounts for all the important features, would be highly welcome.

Whereas *ab initio* methods can convince because of their excellent results, they do not provide models that help to visualize or get an intuitive feeling for the processes involved. Therefore, our aim was to close this gap and provide a more intuitive model. In the following, the objectives and choices for such models are discussed.

With *ab initio* methods at a fairly advanced state, it is possible to close a gap between experiment and theory. Since the predictive powers of DFT are proven by testing them *versus* experimental results on accessible systems, the stage is set to do "computer experiments" on non-accessible systems. Real experiments are of course of higher validity. Nevertheless, it is much better to do calculations, than having no way to get any information on these systems. Especially when using the output to parameterize classical models, it is perfectly consistent to use *ab initio* results instead of experimental numbers.

We chose to study Sodium-Fluoride clusters, since classical models proved to be especially easy and useful for Alkali-Halide systems. Furthermore there exists a rather broad range of experimental results available for small molecules of this type.

Our objective was to use quantum mechanics to examine the evolution of the cluster properties as size increases, and also to make a classical model for molecular dynamics simulations on medium-sized systems. Since it proved that quantum effects are too important and diverse, the latter goal had to be modified during the course of this work.

The outcome is a thorough DFT study of NaF systems in chapter 2, where we try to illuminate the basic reasons for the calculated structures and their properties, and then a short discussion of classical models in chapter 3.

Chapter 2

A study of small Sodium-Fluoride clusters with DFT

2.1 Introductory remarks

In the present chapter we report the results of computations performed with NRLmol. We start with a study of the four important single-nuclei cases (Na, Na^+, F, F^-), then go on to NaF and finally to larger clusters. In order to make full use of the results it is necessary that we first illustrate the relation between the computed values and their real physical meaning.

Geometric parameters, i.e. positions of the nuclei:

As mentioned earlier, all DFT results are for the ground state of the system. On the other hand, experimental techniques might require higher temperatures (e.g. for gas phase experiments of NaF). Then the experimental bond length is higher due to anharmonic vibrations of the molecule, and corrections are necessary [11]. In this work all cited experimental results are corrected so as to be directly comparable to the DFT numbers, unless stated otherwise.

Polarizabilities:

We get the polarizability matrix $\hat{\alpha}$ from DFT by applying an external electric field $\mathbf{F}$ ($\mathbf{F}$, to avoid confusion with the energies) and looking at the change of the dipole moment $\boldsymbol{\mu}$ of the system. The coefficients of the linear term in $\mathbf{F}$ are then the elements of the tensor:

$$\alpha_{ik} = \frac{\partial \mu_i}{\partial F_k} \tag{2.1}$$

For the considered systems we distinguish the purely electronic α_e from the total polarizability α_{tot}. In the first case we keep the positions of the nuclei fixed while applying the field (experimentally, this corresponds to high frequency electric fields), whereas in the second case we let them relax in the field.

Another important result comes from quantum mechanical perturbation theory and will be used to interpret the DFT results. With the unperturbed many-particle Hamiltonian H of the electronic system and its non-degenerate eigenvalues $E_n^{(0)}$ with eigenfunctions $|n^{(0)}\rangle$, where n= 0 represents the ground state, we get the electronic polarizability matrix in first order approximation. It only depends on the dipole transition elements between all other states and the ground state and their corresponding energy differences.

The field **F** creates a perturbation term V in the Hamiltonian:

$$V = -\sum_{k=1}^{3} F_k \mu_k \quad with \quad \mu_k \equiv \sum_i q^i x_k^i \tag{2.2}$$

The second sum goes over all electrons. If we wanted to get the total polarizability we additionally would have to take account of the core motion. Now we introduce the notation $\langle k^{(0)}|A|n^{(0)}\rangle = \langle A \rangle_{kn}$ and use the first order perturbed wavefunctions $|n^{(1)}\rangle$,

$$\left| n^{(1)} \right\rangle = \left| n^{(0)} \right\rangle + \sum_{\lambda \neq n} \left| \lambda^{(0)} \right\rangle \frac{\langle V \rangle_{\lambda n}}{E_n^{(0)} - E_\lambda^{(0)}} \tag{2.3}$$

to compute the electronic dipole moment μ along direction x_i.

$$\mu_i(\vec{F}) = \langle \mu_i \rangle_{nn} + \sum_{k=1}^{3} \sum_{\lambda \neq n} \frac{-F_k \left(\langle \mu_i \rangle_{n\lambda} \langle \mu_k \rangle_{\lambda n} + c.c. \right)}{E_n^{(0)} - E_\lambda^{(0)}} \tag{2.4}$$

By using (2.1) we get the desired expression for the polarizability matrix elements, here with n= 0 for a system which is in the electronic ground state:

$$\alpha_{ik} = \sum_{\lambda > 0} \frac{\left(\langle \mu_i \rangle_{0\lambda} \langle \mu_k \rangle_{\lambda 0} + c.c. \right)}{E_\lambda^{(0)} - E_0^{(0)}} \tag{2.5}$$

Special care has to be taken when comparing the so-called free ion results with experiment, as many experimental values are obtained by refraction experiments on crystals and by making several assumptions, which make it doubtful whether this value corresponds to the real free ion. We will come back to that topic when discussing the free ion polarizabilities.

Vibrational frequencies:

NRLmol computes the force constants of the system by small displacements of the nuclei. With that information the eigenvalue equation for the vibrational frequencies can be solved. In addition information about the infrared (IR) and Raman-activity of every mode is gained. We can also use group theory to get information about the geometrical shape of those modes [12].

2.2 The single nuclei cases Na, Na$^+$, F, F$^-$

2.2.1 Energies

The purpose of starting with the simplest systems is also to get a feeling for the different options in DFT. We will compare the effect of using different exchange-correlation functionals and of including spin effects into the computations. Spins are always important in cases where at least one orbital is only singly occupied, as the other electrons will then feel the uncompensated magnetic moment of this electron. In the present case this means we have to use spin-density for the two neutral atoms Na and F.

TABLE 2.1:
NRLmol **ground state energies in Hartrees with respect to free electrons and nuclei**

	Na	Na$^+$	F	F$^-$
GGA without spin σ	-162.162	-161.973	-99.649	-99.804
GGA with spin σ	-162.170	-161.973	-99.664	-99.804
LDA with spin σ	-161.443	-161.246	-99.111	-99.259

As we can see in Table 2.1 the inclusion of spins does not make a difference for the ionic cases. This has the consequence that it is essential to include the spins when computing ionization energies or electron affinities as can be seen in Table 2.2. We also use those energies to better compare the differences of the two E_{xc}-functionals. The total energies cited in those tables are in relation to free electrons and nuclei. In contrast to the energies of the single particle DFT energy levels, they are theoretically fully justified and can be

compared to experiment. Accordingly we get the ionization energies by taking the difference between two separate calculations, one on the neutral atom and one on the ion, and not by simply taking the HOMO energy of the neutral atom.

TABLE 2.2:
Ionization energy and electron affinity in eV with NRLmol

	GGA (no σ)	GGA (σ)	LDA (σ)	Experiment [13]
Na ionization energy	5.14	5.35	5.36	5.14
F electron affinity	-4.21	-3.81	-4.02	-3.40

2.2.2 Polarizabilities

First we want to compare the polarizabilities with and without spins and also for the different functionals to improve our estimation of the differences arising from our choice. Whenever we compute them, we use sufficiently weak electric fields in order that, in the dipole moment, only the linear term in the E-field is important. As already mentioned in the introduction, the experimental values for the ions do not correspond to what was computed here. Experimentally one merely gets the polarizability for one formula unit of the crystal by doing refraction experiments upon it and then using the Clausius-Mossotti relation:

$$\alpha_{electronic} = \frac{3}{4\pi\rho} \frac{\varepsilon_\infty - 1}{\varepsilon_\infty + 2}$$

(2.6)

Applying high-frequency fields, we get the electronic polarizability from the dielectric constant. Then the assumption is made that this result equals the sum of the electronic polarizabilities of the two ions [14]. This method misses two important points:

1) The ionization in the crystal might not be perfect, which means that it might make sense to assign non-integer charges to the ions, corresponding to hybrid-orbitals shared by multiple ions. As a consequence α might change drastically from free ion values.

2) The general form of the orbitals and their energies might have changed. From the QM expression for α we can see that this results in differences from the free ion value.

This does not mean that the experimental results are not useful, we simply propose to handle them with more care and not to designate them as free ion polarizabilities.

For the neutral atoms the experiment truly measures α for the gas phase and therefore directly corresponds to our results. This technique uses an atom interferometer to

measure the phase shift in atomic beams induced by the quadratic Stark effect. The error bars in those experiments are very small, but we only have results for free Na [15] and not for F.

TABLE 2.3:
Polarizabilities α of the single nuclei in 10^{-24} cm³

	Na	Na$^+$	F	F$^-$	Na$^+$+F$^-$
GGA (no σ)	22.59	0.144	0.536	1.23	
GGA (σ)	23.18	0.144	0.536	1.23	1.37
LDA (σ)	20.71	0.158	0.538	1.22	
experiment	24.11(6) [15]	0.37* [14]		0.85* [14]	1.22
Hartree-Fock perturbation theory [16]		0.140		1.40	

* From crystal refraction. There is broad range of values in the literature (e.g. 0.76-0.98 for F⁻, see [14]). We should only take the sum $\alpha_{Na+}+\alpha_{F-}$ and compare it to calculations on crystal structures, but not to the free ion values in this table!

In the present case α reduces to a scalar, because the systems have cubic symmetry. Since we do not have more experimental results, the only number which is reliable for comparison is the free Na result. Overall we see a physically satisfying tendency that DFT results improve if we include spins for systems where it is necessary. Also, as generally agreed upon by DFT experts, the errors coming from the E_{xc}-functional decrease for GGA compared to LDA. Later in this work we will always use GGA and include spins whenever necessary.

Now we want to find an explanation for the remarkably high α for Na, which is increased by more than a factor of 10^2, just by adding an electron to Na$^+$. On the other hand, the change between F and F⁻ is only a little more than a factor of 2. If we look at the QM perturbation expression for α (2.5), it becomes obvious that there are three different reasons for changes in α:

1) Changes in the energy differences of the electron orbitals. As we are adding an electron to the system, they will be smaller and this results in an increase of α. This effect takes place in both F and Na alike.

2) Modification of the matrix elements of μ. No overall tendency can be seen here, as orbitals in general will contract, but not in a unique fashion. Especially the inner occupied levels will not contract very much. Therefore no prediction for the change of $\langle \mu \rangle$ can be made.

3) The newly occupied level in Na has the effect of deleting terms from the sum in (2.5), namely those which had this level as final state in a transition. Equally, it

creates new terms which start from this new orbital. In F we do not get any fundamental change, as the new electron in F⁻ occupies the last of the 2p states. This deletes the transitions starting at 1s and 2s going to that state, which do not have very large dipole moments anyway, and it creates more transitions starting at 2p. Since there were already 5 electrons occupying those orbitals we only expect a change by approximately a factor of 6/5. For Na things are different. The 3s state which is now occupied in contrast to Na⁺ has a huge dipole transition to the 3p states. If we look at the strong Na D-lines in the solar spectrum, we could already have expected this.

We also want to check this theory with our DFT calculations. In chapter 1 we emphasized that we should not give physical meaning to the Kohn-Sham energies and electron orbitals. Nevertheless, as we can see from (1.17), most of the error we made cancels if we only consider energy differences. Consequently we calculated the contribution of the 3s to 3p transition of the Na polarizability in the framework of DFT.

That means we calculated $\langle\mu\rangle_{3s\rightarrow3p}$ with the Kohn-Sham orbitals and $\Delta E_{3s\rightarrow3p}$. With our results $\langle\mu\rangle_{3s\rightarrow3p}$= 2.480 ea_B and $\Delta E_{3s\rightarrow3p}$= 0.0784 Hartree, we get a contribution from this transition to the total polarizability of $\alpha_{Na,3s\rightarrow3p}$= 23.2 10^{-24} cm³. This supports our explanation especially as all other dipole moments were much smaller. It is also remarkable that our energy difference is very close to what we get from experiments. A comparison shows that our value $\Delta E_{3s\rightarrow3p}$= 2.13 eV reproduces the experimental energy of the Sodium D-lines $E_{Na,D}$= 2.11 eV up to a small error. This and the very good reproduction of α is of course not what one can normally expect from DFT. Much more important is the information that α is really dominated by one transition alone.

A check of the dipole transition elements and their corresponding energies for F gives the result that many transitions contribute to α and no single transition dominates.

Another interesting question concerns the two isoelectronic ions Na⁺ and F⁻. Since they both have 10 electrons, their shells with n= 1,2 are fully occupied and all the transitions that bring important contributions to α are between states with n= 2 → n= 3. This enables us to make a simple prediction of the ratio of those two polarizabilities. As the electrons occupy the same states, we only need to estimate the average change in the energy differences and the dipole moments for the important transitions. To estimate the energy differences we use the paradigm of the hydrogen atom. First we look at the simple result for the energy levels, which we get from QM by using only electrostatic energy:

$$E_n = -\frac{Z^2}{n^2} \quad \text{(in atomic units)} \tag{2.7}$$

Instead of using (2.7) to calculate the energy differences we have to take the shielding of the core charge by the other electrons into account. The simplest formula that is used to model the experimental energies of the L_α-lines is exactly what corresponds to our case. It is [17]:

$$E_{L_\alpha} = \frac{5}{36}(Z - 7.4)^2 \quad \text{(in atomic units)} \tag{2.8}$$

We have to compare the cases Z= 9 and Z= 11. Accordingly we get a ratio in the energy differences of about 5. We can compare this factor of 5 with the energy levels we get from DFT.

TABLE 2.4:

Kohn-Sham energies of ionic orbitals, computed with NRLmol, in Hartree

	E(2s)	E(2p)	E(3s)	E(3p)	ΔE(2s→3p)	ΔE(2p→3s)
Na$^+$	-2.36	-1.34	-0.266	-0.147	2.09	1.19
F$^-$	-0.596	0.0729	0.399	0.465	1.06	0.326

As can be seen in Table 2.4, this factor is not very exact. Since we only want to make a simple estimate, let us choose a factor of 4. Following this $\alpha(F^-) \cong 4\,k\,\alpha(Na^+)$, where k has to take the ratios of the dipole moments into account. The remaining factor tells us that α gets another enhancement in F$^-$ from larger dipole moments. Looking at hydrogen we can at least qualitatively understand this, since the distances scale with $1/Z^2$ for heavier cores. Due to shielding this is of course modified. Nevertheless the Na$^+$ orbitals are more compressed and therefore all integrals, including the dipole moments are scaled. Fitting k to the polarizabilites we get the following ratio for the dipole moments (approximate relation for all states important for the transition):

$$1.46 \left\langle \mu \right\rangle_{Na+} \cong \left\langle \mu \right\rangle_{F-} \tag{2.9}$$

Later on this approximation will be used for explaining the nonlinearities in α.

2.2.3 Nonlinear induced dipole moments

So far we only applied small external electric fields, which gives a linear relation between the **F**-field and induced dipole μ. This approximation loses its validity as soon as higher terms in **F** become important. Strictly speaking, instead of using (2.1) we should start with the more general relation:

$$\vec{\mu}(\vec{F}) = \vec{\mu}_0 + \hat{\alpha}^{(2)}\vec{F} + \frac{1}{2}\vec{F}\hat{\alpha}^{(3)}\vec{F} + ... \tag{2.10}$$

It becomes obvious that our definition of α, which was the matrix $\hat{\alpha}^{(2)}$, has to be modified for higher fields. For this reason we define the polarizability of an object in an external electric field as the linear coefficient in the expansion series around this very field. Thus we get the generalized version of (2.1):

$$\hat{\alpha}(\vec{F}_{ext}) \equiv \left. \frac{\partial \vec{\mu}(\vec{F})}{\partial \vec{F}} \right|_{\vec{F}=\vec{F}_{ext}} \qquad (2.11)$$

In the case of molecules it is important to keep in mind that we are dealing with external fields, i.e. the internal fields are not considered here. This is crucial because the internal fields normally exceed the external ones by multiple orders of magnitude. For simplicity of notation let α denote the case when in the limit of $\mathbf{F}_{ext} \rightarrow 0$.

Having discussed the theoretical aspect of this phenomenon we will now go on to the results of a calculation on the F$^-$-ion in an external **F**-field.

Fig. 2.1: Dipole moment μ of the Fluoride ion in an external field.
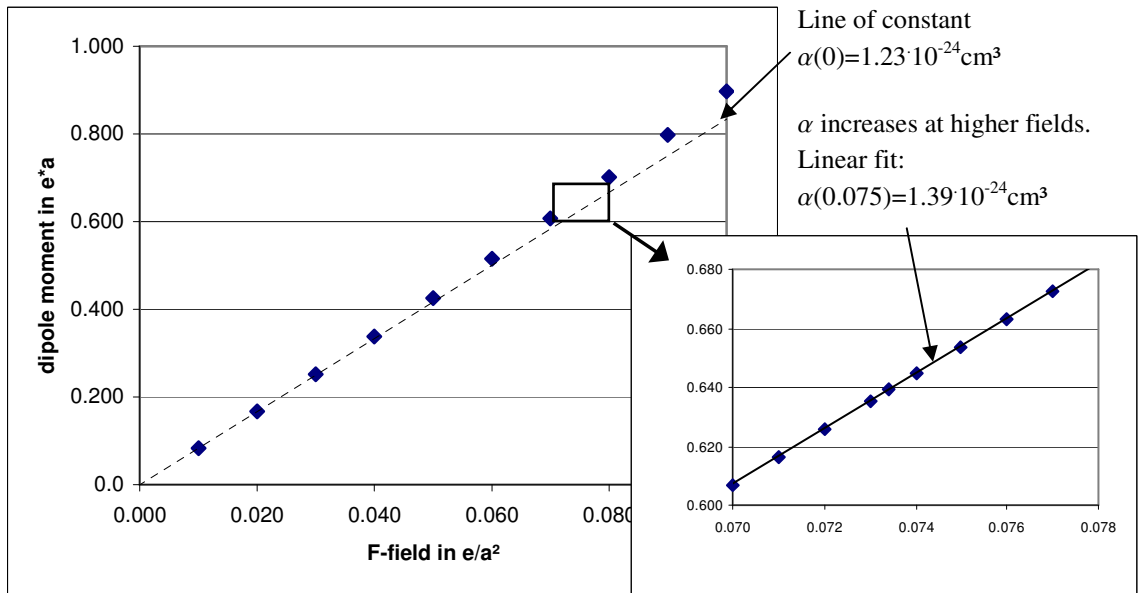
As can be seen in Fig. 2.1 the behaviour of μ becomes in fact nonlinear for fields above ~10^{-2} e/a². Accordingly, for truly external fields (which means not created by neighbouring ions), the linear approximation is fully justified here, as $1e/a_B^2 = 5.15 \cdot 10^{11}$ V/m. Fields created during experiments are well below the threshold for detecting nonlinearity. Still, especially when keeping quasi-classical models in mind, the nonlinear effects become important. Looking at the magnified part of the graph in Fig. 2.1 we see the behaviour at a field strength equal to that created by a point charge of 1e at a distance d=3.64a$_B$ (which

equals the experimental bond length of NaF). Here α is increased by a factor of 11.2%. It has to be remarked, that the purpose of citing α to four digits here is not that we think it is that exact. We only want to get good numbers for internally comparing them and getting the enhancement with reasonable accuracy.

$$\alpha_{F^-}(0) = 1.234 \cdot 10^{-24}\,\text{cm}^3 \qquad \rightarrow \qquad \alpha_{F^-}(0.074) = 1.385 \cdot 10^{-24}\,\text{cm}^3 \qquad (2.12)$$

This enhancement effect might be relevant when conceiving simplifying models which are to be used for chemical calculations, as we will try to do in chapter 3. It should also be kept in mind as a phenomenon that always has to be considered when thinking about polarizabilities.

We did the same calculation for our second ion Na^+, and found that the effect is not as profound as for F^-; only an increase of 0.9%.

$$\alpha_{Na^+}(0) = 0.1445 \cdot 10^{-24}\,\text{cm}^3 \qquad \rightarrow \qquad \alpha_{Na^+}(0.074) = 0.1458 \cdot 10^{-24}\,\text{cm}^3 \qquad (2.13)$$

An understanding of this smaller enhancement can again be gotten by looking at perturbation theory. First of all we have to realize that for symmetry reasons μ has non-vanishing coefficients only for odd terms in $\mathbf{F}_{ext}$, because $\mu(\mathbf{F}) = -\mu(-\mathbf{F})$. This means that the first variation in α is quadratic in $\mathbf{F}_{ext}$. Accordingly we write for both ions:

$$\alpha(F) = \alpha(0) + \frac{1}{2}\beta F^2 \qquad (2.14)$$

β is often called hyperpolarizability. As a second step the expression in perturbation theory that corresponds to β has to be found. $\alpha(0)$ is already given by (2.5), and β can be retrieved from 3rd order perturbation theory. Getting the ratio of $\beta(F^-)/\beta(Na^+)$ is all we want. This means we do not have to worry about constant prefactors.

$$\beta \propto \sum_{m \neq n} \sum_{l \neq n} \sum_{k \neq n} \frac{\langle \mu \rangle_{nm} \langle \mu \rangle_{ml} \langle \mu \rangle_{lk} \langle \mu \rangle_{kn}}{(E_n - E_m)(E_n - E_l)(E_n - E_k)} \qquad (2.15)$$

Formula (2.15) is what comes from time-independent perturbation theory. The states we sum over are the same for both ions, and again the approximation from formulas (2.8) and (2.9) is used. Doing this we get a simple estimation:

$$\frac{\beta(F^-)}{\beta(Na^+)} \cong 4^3 \cdot 1.46^4 \cong 290 \qquad (2.16a)$$

From (2.12) and (2.13) we can also get this ratio, with the result:

$$\frac{\beta(F^-)}{\beta(Na^+)} \cong \frac{1.385 - 1.234}{0.1458 - 0.1445} \cong 120 \qquad (2.16b)$$

18

Of course (2.13) and (2.14) are not exactly the same, but nobody would have expected this from such a simple model and the very empirical way of getting the constant in (2.9). Nevertheless we can get a qualitative understanding for the much lower enhancement of α in the Sodium ion compared to the isoelectronic Fluoride ion. It has to be emphasized again, that this explanation can of course make no prediction of the absolute value of α or β but gives a qualitative understanding of their ratios because of their equal number of electrons.

2.3 The NaF monomer

We dedicate a separate subchapter to the special case of the diatomic molecule, the "monomer" (dimer would then be Na_2F_2, etc.). There are two reasons for doing that. First, it is the only case apart from the bulk crystal where we have an abundance of experimental results and thus it provides another thorough check for the NRLmol code. Second, we will try to understand it as well as possible, since the monomer is one end of the broad range of clusters which ends at the crystal. Doing this we are always remembering that we will try to find a quasi-classical model in chapter 3.

TABLE 2.5:
Summary of the NaF monomer parameters

	NRLmol	Exp. [18]	Exp. [19]	Theory [20]	Theory [21]
d [a_B]	3.69	3.64	3.64	3.64	3.62
μ [$e^{\cdot}a_B$]	3.07	3.21			
$\tilde{\nu}[cm^{-1}]$	510	536	536	545	541
$\alpha_{elec., \perp}$ [10^{-24}cm³]	2.39				
$\alpha_{elec., \parallel}$ [10^{-24}cm³]	3.33				
$\alpha_{total, \parallel}$ [10^{-24}cm³]	4.19				

Before giving details of the different calculated values, we start with an overview of the results in comparison with experiment and other theoretical calculations. A discussion is in the subsequent sections. Again, it proved impossible to find experimental data for α. This might partly be due to the fact, that in experiments we also get contributions from the orientation of the static dipole in an external field, which are not included in the

NRLmol result. This statistical Debye-Langevin polarizability α_{DL} only depends on the static dipole and the temperature. For small electric fields (and for the usual temperatures which are larger than the rotational quantum of energy) it is given by:

$$\alpha_{DL} = \frac{\mu_{tot}^2}{3k_B T} \tag{2.17}$$

In addition the anisotropy of α might be hard to take into account experimentally, since we cannot expect to find it in gas phase experiments.

On the other hand, the experimental bond length and vibrational frequency are well established and therefore reliable for comparison. The NRLmol value for the bond length is about 1.5% higher than experiment, whereas the vibrational frequency lies about 5% below the experimental result.

2.3.1 Perturbation theory on diatomic molecules

As previously, we use quantum mechanical perturbation theory to get a physical understanding of NaF. The theoretical framework developed here can be applied to any diatomic system by just changing the core charges and the number of electrons.

Using Born-Oppenheimer approximation, we split the Hamiltonian into an electronic Hamiltonian H_e and a Hamiltonian for the cores H_c. H_e, which contains the positions of the cores only as parameters, will be solved with DFT. The other Hamiltonian H_c will then be solved classically. It involves the electrons through their total energy, which enters H_c as a function of core positions only.

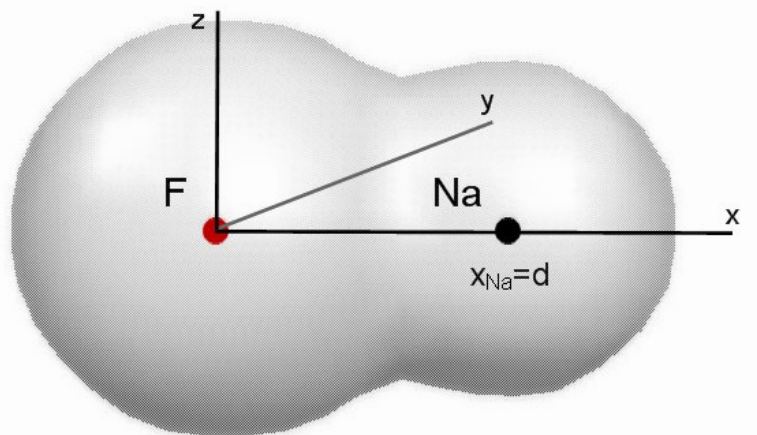Fig. 2.2: Schematic depiction of the NaF monomer

Fig. 2.2 defines the coordinate system and the bond length d. Finally we write down the two Hamiltonians:

$$H_e = \sum_{all\ electrons\ i} \left(\frac{p_i^2}{2m_e} + \sum_{j \neq i} \frac{1}{2} \frac{e^2}{|\vec{r}_i - \vec{r}_j|} - \frac{q_F e^2}{|\vec{r}_i|} - \frac{q_{Na} e^2}{|\vec{r}_i - d\vec{e}_x|} \right) \tag{2.18}$$

$$H_c = \frac{P_{Na}^2}{2m_{Na}} + \frac{P_F^2}{2m_F} + \frac{q_{Na}q_F e^2}{d} + E_0(d) \quad with \quad H_e|0\rangle = E_0(d)|0\rangle \tag{2.19}$$

We emphasize again the general procedure. After solving (2.18) we look classically for the minimum of (2.19), which gives the total energy, the bond length and the electron density via (2.18).

   The physically interesting effects are now the application of an electric field and a variation in the bond length. Of course the first effect will presumably create the second one and it will be worth knowing in which way. For simplicity let us start with a mere variation of the bond length. We now denote the equilibrium bond length with d_{eq} and look at small variations Δd of the Na x-coordinate. Since the total energy has no linear change in Δd, but only a quadratic one, we Taylor-expand up to second order. This also gives interesting information about the linear terms.

$$\Delta H_e(\Delta d) = \sum_{all\ electrons\ i} \left(\frac{q_{Na} e^2}{|\vec{r}_i - d_{eq}\vec{e}_x|} - \frac{q_{Na} e^2}{|\vec{r}_i - (d_{eq} + \Delta d)\vec{e}_x|} \right)$$

$$\cong \sum_{all\ electrons\ i} \left(\frac{q_{Na} e^2 (d_{eq} - x_i)}{|\vec{r}_i - d_{eq}\vec{e}_x|^3} \Delta d + (-\frac{1}{2} q_{Na} e^2) \left(3 \frac{(d_{eq} - x_i)^2}{|\vec{r}_i - d_{eq}\vec{e}_x|^5} - \frac{1}{|\vec{r}_i - d_{eq}\vec{e}_x|^3} \right) \Delta d^2 \right)$$

$$\equiv H_{e1} \cdot \Delta d + \frac{1}{2} H_{e2} \cdot \Delta d^2 \tag{2.20}$$

That implies for the first order:

$$E_0(d_{eq} + \Delta d) = E_0(d_{eq}) + \langle H_{e1} \rangle_{00} \Delta d \tag{2.21}$$

Because x averaged over all electrons is less than d_{eq}, $\langle H_{e1} \rangle_{00}$ has the same sign as Δd. Thus for increased bond length the electronic energy also increases and vice versa. This first order effect has to be cancelled exactly by a change in the core-core repulsive energy, since the expansion is around the energy minimum.

$$\frac{q_{Na}q_F e^2}{d_{eq} + \Delta d} \cong \frac{q_{Na}q_F e^2}{d_{eq}} - \frac{q_{Na}q_F e^2}{d_{eq}^2} \Delta d + \frac{1}{2} \frac{q_{Na}q_F e^2}{d_{eq}^3} \Delta d^2 \tag{2.22}$$

Consequently we arrive at the following equation:

$$-\frac{q_{Na}q_F e^2}{d_{eq}^{\,2}}+\left\langle H_{e1}\right\rangle_{00} \equiv 0 \tag{2.23}$$

Finally the harmonic expansion of the total energy can be written in the following way:

$$E_{tot} \cong E(d_{eq})+\frac{1}{2}\lambda\,\Delta d^2 \quad with \quad \lambda=\frac{q_{Na}q_F e^2}{d_{eq}^{\,3}}+\left\langle H_{e2}\right\rangle_{00}+2\sum_{k>0}\frac{\left|\left\langle H_{e1}\right\rangle_{0k}\right|^2}{E_0(d_{eq})-E_k(d_{eq})} \tag{2.24}$$

Here it is essential to realize that there are two separate expansions. The first one is in the electronic Hamiltonian for small Δd and the second one is the quantum mechanical perturbation theory. As a result, there are two terms in (2.24) originating from the electronic energy.

Related to the displacement of atoms is the concept of dynamical charges as explained in [22]. This question arises when one formally wants to assign charges to individual atoms in compound systems. One way of doing this, which always retains some arbitrariness, is to assign static charges in molecules. Following this concept a boundary has to be drawn and electrons or electron densities have to be distributed amongst the atoms. For our case of the monomer we use the following simple definition for the static charge Z:

$$Z(d) \equiv \frac{\mu(d)}{d} \tag{2.25}$$

In order to have a transferable definition the unambiguous concept of the dynamical charge Z* is introduced. It is defined via the change of the dipole moment μ with a variation of the atomic positions. For the case of the diatomic molecule we get:

$$Z*(\tilde{d}) \equiv \left.\frac{\partial\mu(d)}{\partial d}\right|_{d=\tilde{d}} = Z(\tilde{d})+\tilde{d}\left.\frac{\partial Z(d)}{\partial d}\right|_{d=\tilde{d}} \tag{2.26}$$

It differs from the static charge by an additional term which takes account of the change of Z with bond length. Another important fact is that our definition of Z* is for zero external electric field. Consequently that has to be taken into account when making comparisons, as experimentally one achieves a change of bond length by applying an **F**-field. For completeness and further use, we also write the corresponding quantum mechanical expressions for (2.25) and (2.26) at d= d_{eq}, by using the eigenvector definitions of (2.19).

$$Z(d) = \frac{1}{d}\left\langle\mu_x\right\rangle_{00}+q_{Na} \tag{2.27}$$

$$Z*(d) = \frac{\partial}{\partial d} \langle \mu_x \rangle_{00} + q_{Na} = \sum_{k>0} \frac{\langle \mu_x \rangle_{0k} \langle H_{e1} \rangle_{k0} + c.c.}{E_0 - E_k} + q_{Na} \qquad (2.28)$$

The definition of the electronic dipole operator is the same as in (2.2).

Let us now look at the effects of an electric field. Keeping the ions fixed, we can get the electronic polarizabilities according to (2.5). By symmetry, the off-diagonal elements are all zero and $\alpha_{xx} \neq \alpha_{yy} = \alpha_{zz}$. Of course the most interesting case is a field in x-direction, since the bond length will change if the nuclei relax. This is the first effect we want to look at. The change in the electronic Hamiltonian is now a function of Δd and F_x.

$$\Delta H_e(\Delta d, F_x) = H_{e1} \cdot \Delta d + \frac{1}{2} H_{e2} \cdot \Delta d^2 - F_x \cdot \mu_x \qquad (2.29)$$

This means that the change in the core Hamiltonian H_c becomes:

$$\Delta H_c(\Delta d, F_x) = -\frac{q_{Na} q_F e^2}{d_{eq}^2} \Delta d + \frac{1}{2} \frac{q_{Na} q_F e^2}{d_{eq}^3} \Delta d^2 - F_x q_{Na}(d_{eq} + \Delta d) + \langle \Delta H_e(\Delta d, F_x) \rangle \qquad (2.30)$$

After writing the whole Hamiltonian, we again want a formula like (2.24) for the total energy. Wishing to expand to second order, terms in Δd and F_x are treated as same order. Then we can find the new minimum of the total energy as a function of Δd. This way we also get the desired relation $\Delta d(F_x)$. Before doing that we have to evaluate the expectation value in (2.30):

$$\langle \Delta H_e(\Delta d, F_x) \rangle = \langle H_{e1} \rangle_{00} \Delta d - F_x \langle \mu_x \rangle_{00} + \frac{1}{2} \langle H_{e2} \rangle_{00} \Delta d^2 + \sum_{k>0} \frac{\left| \langle H_{e1} \Delta d - F_x \mu_x \rangle_{0k} \right|^2}{E_0(d_{eq}) - E_k(d_{eq})} \qquad (2.31)$$

The last term still needs to be simplified, but it can be seen that it can be re-expressed using the dynamical charge $Z*$ and the electronic polarizability α_{xx}.

$$\sum_{k>0} \frac{\left| \langle H_{e1} \Delta d - F_x \mu_x \rangle_{0k} \right|^2}{E_0(d_{eq}) - E_k(d_{eq})} = \sum_{k>0} \frac{\left| \langle H_{e1} \rangle_{0k} \right|^2}{E_0(d_{eq}) - E_k(d_{eq})} \Delta d^2 - F_x \Delta d(Z* - q_{Na}) + \frac{1}{2} F_x^2 \alpha_{xx} \qquad (2.32)$$

Now we have to collect the terms in formulas (2.30)-(2.32). Two of them cancel according to (2.23), and we will again use our definition of λ from (2.24).

$$E_{tot}(F_x) = E(d_{eq}) - \left(q_{Na} d_{eq} + \langle \mu_x \rangle_{00} \right) F_x + \frac{1}{2} \alpha_{xx} F_x^2 - F_x \Delta d Z* + \frac{1}{2} \lambda \Delta d^2 \qquad (2.33)$$

The second term in this expression is exactly the dipole energy, which means the term in the parenthesis is the total dipole moment μ_{tot} of the unperturbed monomer. To find the new equilibrium distance with **F**-field, we now differentiate with respect to Δd and set the result equal to zero:

$$-F_x Z^* + \lambda \, \Delta d = 0 \quad \rightarrow \quad \Delta d(F_x) = \frac{Z^*}{\lambda} F_x \tag{2.34}$$

With the new equilibrium bond length from (2.34) we get the ground state energy of the molecule depending only on the electric field.

$$E_{tot}(F_x) = E(d_{eq}) - \mu_{tot} F_x + \frac{1}{2}\alpha_{xx}F_x^2 + \frac{1}{2}\frac{(Z^*)^2}{\lambda}F_x^2 \tag{2.35}$$

Last but not least an expression for the total polarizability α_{tot} can be found.

$$\alpha_{tot} = \frac{d\mu_{tot}}{dF_x} = \frac{\partial \mu_{tot}}{\partial d}\frac{\partial d}{\partial F_x} + \frac{\partial \mu_{tot}}{\partial F_x} = Z^*\frac{Z^*}{\lambda} + \alpha_{xx} \tag{2.36}$$

As could have been anticipated, α_{tot} equals the purely electronic polarizability plus some additional factor coming from the movement of the cores, the vibrational polarizability. Remarkably, this additional factor is very simple when using the concept of dynamical charges. Namely, it is proportional to $(Z^*)^2$, which originates in the direct proportionality of Δd and Z^*. We also observe that everything is consistent up to second order, since it can be seen that the coefficient of F_x^2 in the total energy (2.35) is exactly ½ α_{tot}, which is exactly what we would have presumed right from the start.

In the end we found some interesting equations which relate the values we are about to compute. They will provide a very valuable check for future computations and can also be used for other diatomic molecules.

On the basis of this theoretical framework we move on to the discussion of our NRLmol results.

2.3.2 Energy curve and vibration

Before looking at the energy curve depending on separation distance d, we bring back to mind that we are using GGA-functionals and include the electronic spins. For the present case the inclusion of spins presents two different options. What we expect to get is a nonmagnetic state with 10 up and 10 down spins, which doubly occupy the lowest lying orbitals. In principle one can alternatively get a paramagnetic state which has 11 up and only 9 down electrons. Since this state is energetically less favourable, the electrons have to be forced into that spin configuration, but with that accomplished we can also get the energy curve for this spin occupancy.

Fig. 2.3: Energy curve for the NaF nonmagnetic and paramagnetic state
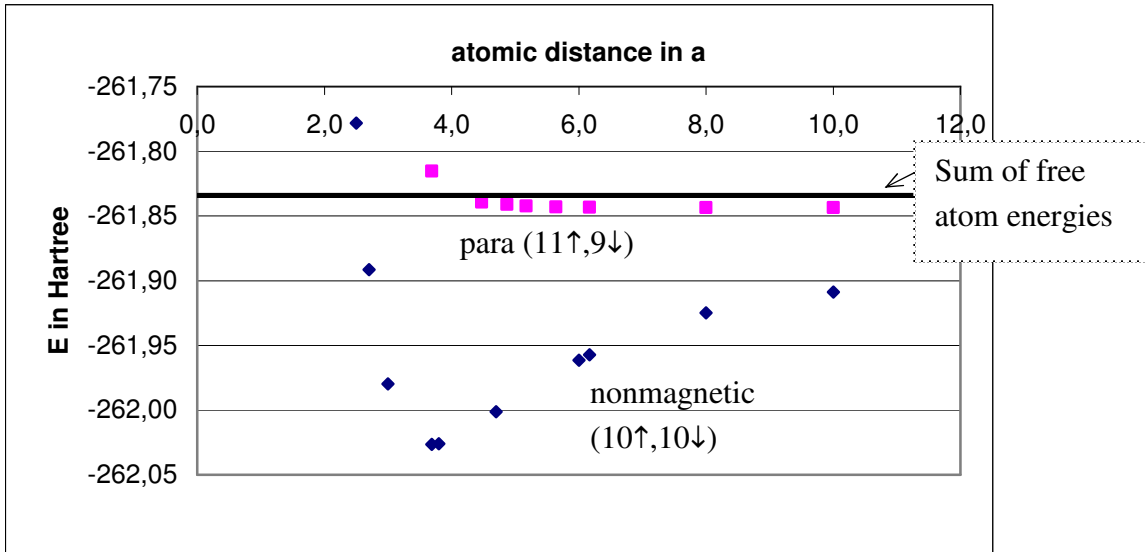
Very clearly it can be seen that the nonmagnetic case is much lower in energy. The minimum lies at a distance of d = 3.69 a_B. At this distance the total energy is:

$$E_{tot} = -262.0266 \; Hartree \tag{2.37}$$

And the paramagnetic state is higher by 5.78 eV. At this distance the paramagnetic state is even higher than the sum of the free atom energies, which can be looked up in the second row of Table 2.1.

From Figure 2.3 we also get information about the dissociation energy of the monomer:

$$theory: \quad E_{diss} = 5.23 eV \quad vs. \, experiment \, [23]: \quad E_{diss} = (5.34 \pm 0.13) eV \tag{2.38}$$

Comparing the dissociation energy with experiment [23] shows that the DFT result is very close, lying within a 5% error-range.

The next interesting energy is the first electronic excitation. Instead of just taking the energy differences between the HOMO and LUMO we do two different computations. The first is just the regular one and in the second we force the highest lying electron to occupy the LUMO and leave the HOMO empty. At the end we take the differences in the total energy between those two results to get the first electronic excitation energy. Table 2.6 shows the result and also compares it to the HOMO-LUMO energy difference.

	E(LUMO)-E(HOMO)	By forced occupancy	Experiment [24]
Different ways to estimate the first electronic excitation energy			
E_1 in eV	3.01	5.57	5.7

Looking at Table 2.6 we see that one needs to do the two separate calculations; the error with the other method is gigantic, while the forced occupancy method produces a result very close to experiment.

Another aspect to look at is the comparison of the perturbation theory results in the last subchapter with direct numerical computations by NRLmol. Using Figure 2.3 it is possible to obtain values for the previously defined variables λ, Z and Z^*. For this purpose we compute the total energy and the dipole moment for a set of distances around the equilibrium distance. What can immediately be writen down with the information in Table 2.5 is the static charge $Z = 0.832$ e.
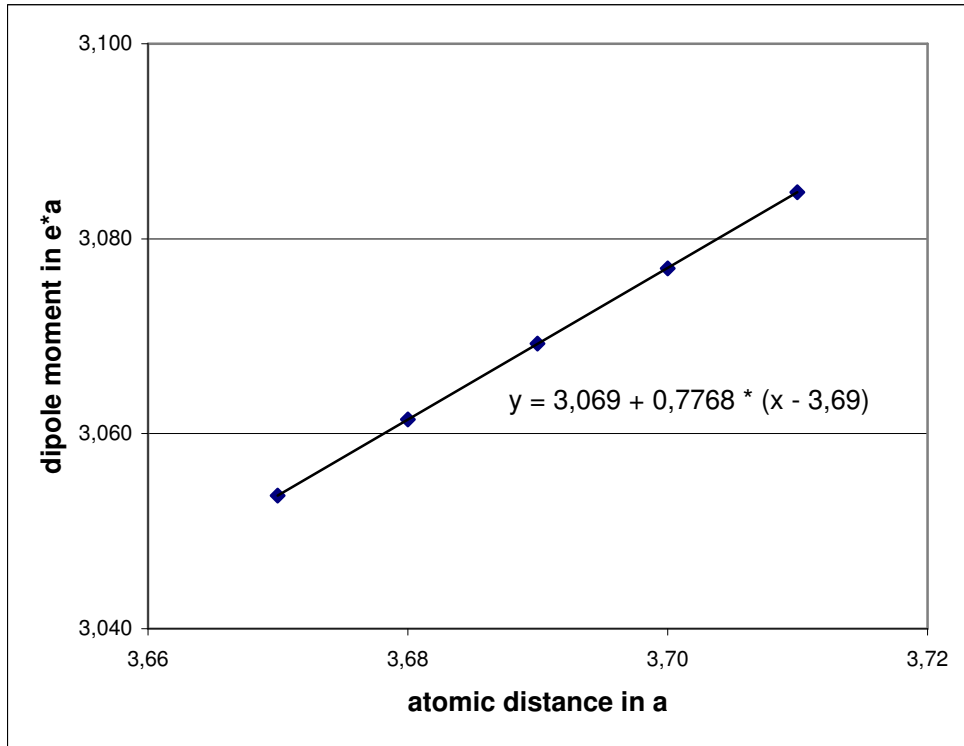
Fig. 2.4: Quadratic least-square fit of the NaF monomer energy around d_{eq} to obtain λ
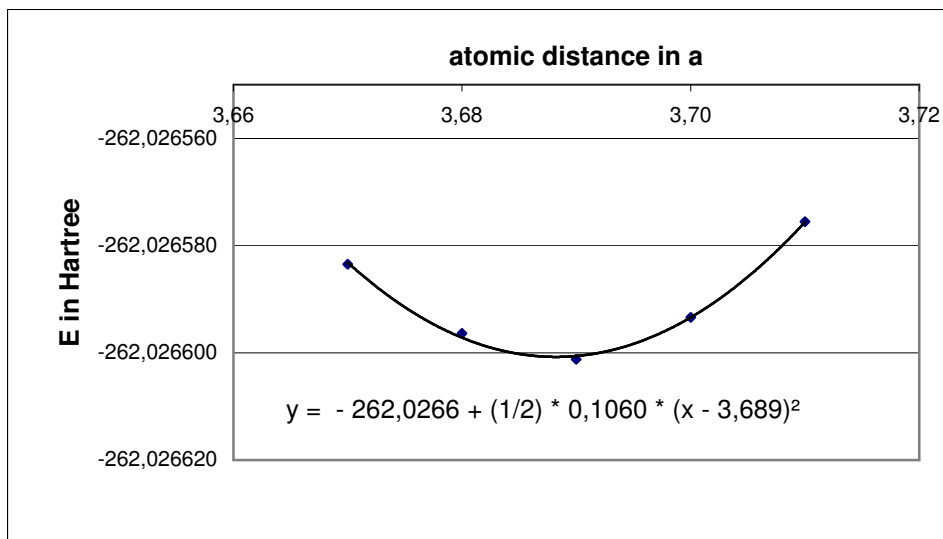
From Figure 2.4 we get λ, which is just the coefficient in front of the quadratic term and from Figure 2.5 Z^*, which is the linear coefficient of the dipole moment.

$$\lambda = 0.1060 \frac{Hartree}{a_B^2} \quad ; \quad Z^* = 0.777e \tag{2.39}$$

Fig. 2.5: Linear least-square fit of the NaF dipole moment around d_{eq}

With this result for λ we can not only check the result for the total polarizability, but also look at the vibrational frequency f. In harmonic approximation, which should be reasonably good for the lowest lying states, the frequency is given by:

$$ f = \frac{1}{2\pi}\sqrt{\frac{\lambda}{m_r}} \quad with \quad m_r = \frac{m_{Na}m_F}{m_{Na}+m_F} \tag{2.40} $$

In the previous formula m_r is the reduced mass, and we also have to relate energies in Hartrees to the atomic mass unit m_0 and one second s. We get the following conversion factor:

$$ \frac{1}{2}m_0\frac{a_B^2}{s^2} = 2.325 \cdot 10^{-48}\,J = 5.339 \cdot 10^{-31}\,Hartree \quad \rightarrow \quad 1\,Hartree = 9.365 \cdot 10^{29}\,m_0\frac{a_B^2}{s^2} \tag{2.41} $$

Using this we write the energy in wavenumbers $\tilde{v} = f/c$ and compare it to Table 2.5. The result of $\tilde{v} = 519\ cm^{-1}$ shows that everything is consistent. The essential part about formula (2.40) is that it provides a way to derive λ from experiments on molecular vibrations.

2.3.3 Polarizabilities

When thinking about the polarizability of the NaF monomer, some questions immediately pop up:

- Why is α enhanced in comparison to the sum of the free ion polarizabilities?
- What is the reason for a bigger electronic α along the molecular axis than perpendicular to it?
- How well does the perturbation prediction for the total polarizability compare with a separate calculation where the molecule relaxes in an external field?

We will discuss and try to explain these problems by using the LCAO bonding picture. This means we will visualize the molecular orbitals (which strictly speaking do not even exist, as only the total wavefunction is theoretically exactly justified) as a linear combination of atomic orbitals. Again we are not aiming for a quantitative understanding, but for the underlying physical mechanisms.

Let us start with the perpendicular electronic polarizability $\alpha_\perp$. The DFT result is $\alpha_\perp =$ 2.39 10^{-24} cm³, whereas $\alpha_{F^-} + \alpha_{Na^+} = 1.37\ 10^{-24}$ cm³. The comparison with the sum of the free ion energies only makes sense if we can really assume the atoms to be fully ionized. NaF is definitely called an ionic compound, especially in the crystalline form.

On the other hand, we have seen in Table 2.5 that the charges we assign are about 20% less than ± 1. Therefore let us try to understand the electronic structure in the LCAO picture. For the free atoms the HOMO in Na is a 3s orbital, represented by the notation $|Na,3s\rangle$. We remember that the high atomic α in the Na atom originated from transitions starting at this orbital. In free F, five of the six 2p states are occupied. This implies that those six electrons have to be redistributed in the NaF molecule.

For the monomer we use the following simple model: The $|F,2p_y\rangle$ and $|F,2p_z\rangle$ states remain unchanged and are both doubly occupied. Thus the remaining task is to find an orbital for the last electron pair. If there were full ionization, we could just say it occupies the $|F,2p_x\rangle$ state. Instead we now create two hybrid orbitals out of the $|Na,3s\rangle$ and the $|F,2p_z\rangle$ states, where the original atomic orbitals are assumed orthonormal. Symmetry requires that p_y or p_z states can never be mixed with s states when making LCAO-orbitals.

$$\left|\gamma-\right\rangle = \kappa\left|Na,3s\right\rangle + \sqrt{1-\kappa^2}\left|F,2p_x\right\rangle$$
$$\left|\gamma+\right\rangle = \sqrt{1-\kappa^2}\left|Na,3s\right\rangle - \kappa\left|F,2p_x\right\rangle \qquad (2.42)$$

κ is a parameter which we fit, so that it reproduces the static charge of the molecule, which is defined in (2.25). We always set $\kappa < 2^{-0.5}$, so that $|\gamma-\rangle$ is lower in energy and therefore doubly occupied, whereas $|\gamma+\rangle$ is our LUMO state. This gives the relation:

$$\kappa^2 = 1 - Z \tag{2.43}$$

In this simple model the explanation for the increased α of NaF compared to the free ions is that again the dipole transition between the hybrid state $|\gamma-\rangle$ and the Sodium p-states is very large. To verify this hypothesis the following test is made:

First we evaluate the transition element $|\langle\gamma-|\mu|Na,3p\rangle|^2 = (1-Z) |\langle Na,3s|\mu|Na,3p\rangle|^2$. Since this last dipole transition is very dominant in Na, this is essentially the contribution to α in NaF which results from transitions on the Sodium atom. For that purpose we formally split the electronic polarizability into two contributions, one from Na transitions and one from F transitions.

$$\alpha_{NaF} \equiv \tilde{\alpha}_{Na} + \tilde{\alpha}_F \tag{2.44}$$

Now we want to re-express the Sodium contribution only in terms of α_{Na} and the differences in energy levels of the participating electron states. As we do internal comparisons and only want to get a qualitative understanding the Kohn-Sham energies of those levels are used. This results in the following formula:

$$\tilde{\alpha}_{Na} = (1-Z)\frac{E(Na,3p) - E(Na,3s)}{E(NaF,Na3p) - E(NaF,\gamma-)}\alpha_{Na} \tag{2.45}$$

In (2.45) the very small contribution from α_{Na+} is neglected. The next task, before we will give verification for this model, is to explain the Fluoride part. Since the electron configuration on the F nucleus is not much changed, we approximately expect this part to be independent of the static charge. Of course it will be different from the free ion α, but constant.

Finally a test has to be made with this simple model. For that purpose we artificially change the bond length and compute $\alpha_\perp$, the static charge and the Kohn-Sham energies. Additionally we need the energies of the Sodium atom orbitals for use in (2.45). Then (2.45) is evaluated for some given bond length d and subtracted from the DFT $\alpha_\perp$ to get the Fluoride contribution according to (2.44). If the model captures the important features, this result should be approximately constant.

Table 2.7 shows that this extremely simple model provides an explanation for the observed phenomenon. The cited polarizability is somewhat smaller than our previous value, because a smaller basis set was used for the calculations of Table 2.7.

Summarizing, the main reason for an increased polarizability in NaF is the non-perfect ionization. This has the effect that contributions from the very large dipole transition ,which is also responsible for the high α in Na, increase the polarizability.

TABLE 2.7:
LCAO model for the NaF perpendicular electronic polarizability depending on the bond length d

d in a_B	$\alpha_\perp(DFT)$ in $10^{-24}\,cm^3$	$1-\dfrac{\mu}{e\cdot d}$	E(NaF,γ-) in hartree	E(NaF,Na3p) in hartree	$\tilde{\alpha}_{Na}$ in $10^{-24}\,cm^3$ see (2.45)	$\tilde{\alpha}_F$ in $10^{-24}\,cm^3$ see (2.44)
3,690	2,155	0,169	-0,195	0,002	1,55	0,61
4,200	2,395	0,175	-0,186	-0,005	1,75	0,65
4,700	2,678	0,181	-0,175	-0,012	2,02	0,66
6,000	3,722	0,219	-0,158	-0,030	3,1	0,62
8,000 *	5,896	0,316	-0,155	-0,048	5,38	0,52

* Results are less reliable for larger separation distances, since it becomes harder to converge the energies. The reason is that the electron density can fluctuate over a large range without resulting in big energy changes.

Figure 2.6:   DFT electronic orbitals of the NaF molecule: HOMO & HOMO-1 are degenerate Fluoride π-states, HOMO-2 is $|\gamma$-$\rangle$ (the third Fluoride π-state mixed with a small $|Na,3s\rangle$ contribution) and LUMO is $|\gamma+\rangle$
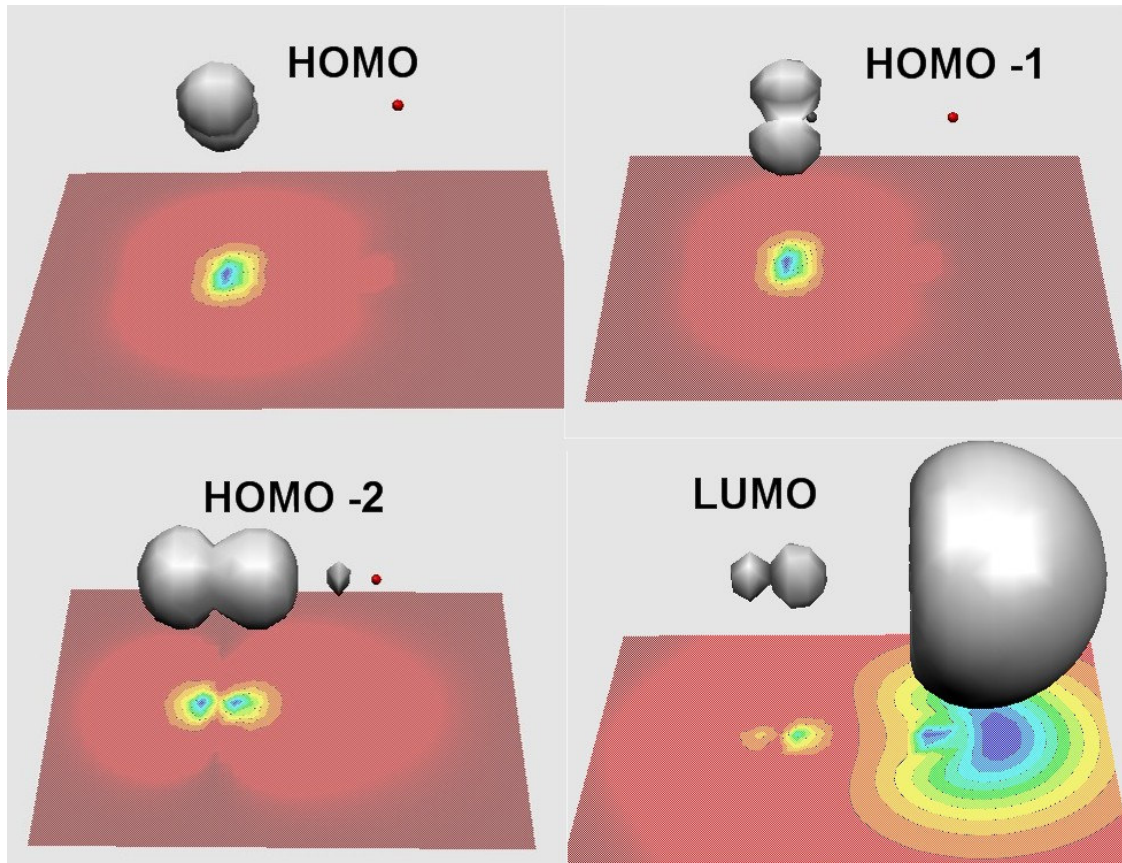
Figure 2.6 and all other graphics of molecules were made with the program Molekel [25,26].

Since Z seems to be the most influential factor on α, an additional test can be made. Let us apply an external electric field at d_{eq}, that results exactly in Z=1. Then $\alpha_\perp$ should decrease and be much closer to the sum of the free ion values.

$$d_{eq}, \; F_x = 0.044 \, Hartree, \; Z = 1 \quad \rightarrow \quad \alpha_\perp = 1.66 \cdot 10^{-24} cm^3 \qquad (2.46)$$

Indeed it decreased and is now only 20% higher than the free ion values, but we also saw in 2.2.3 that α_{F^-} increases with the applied field. Therefore this result additionally supports the model. Taking a look at Figure 2.6, the NRLmol results for some of the electronic orbitals are plotted. The states $|F,2p_y\rangle$ and $|F,2p_z\rangle$ correspond to the HOMO and HOMO-1, whereas the HOMO-2 is the state $|\gamma-\rangle$ and therefore a little bit lower in energy than the other two Fluoride p-states. The planes below the molecule are projection planes for the electron density. In the $|\gamma-\rangle$ projection we can even see the shadow coming from the $|Na,3s\rangle$ contribution. Finally it can be seen that the LUMO is indeed mainly a $|Na,3s\rangle$ state mixed with minor contributions. This is the state $|\gamma+\rangle$.

Fig. 2.7: Electronic dipole moment and $\alpha_{\shortparallel}$ of NaF depending on the external field
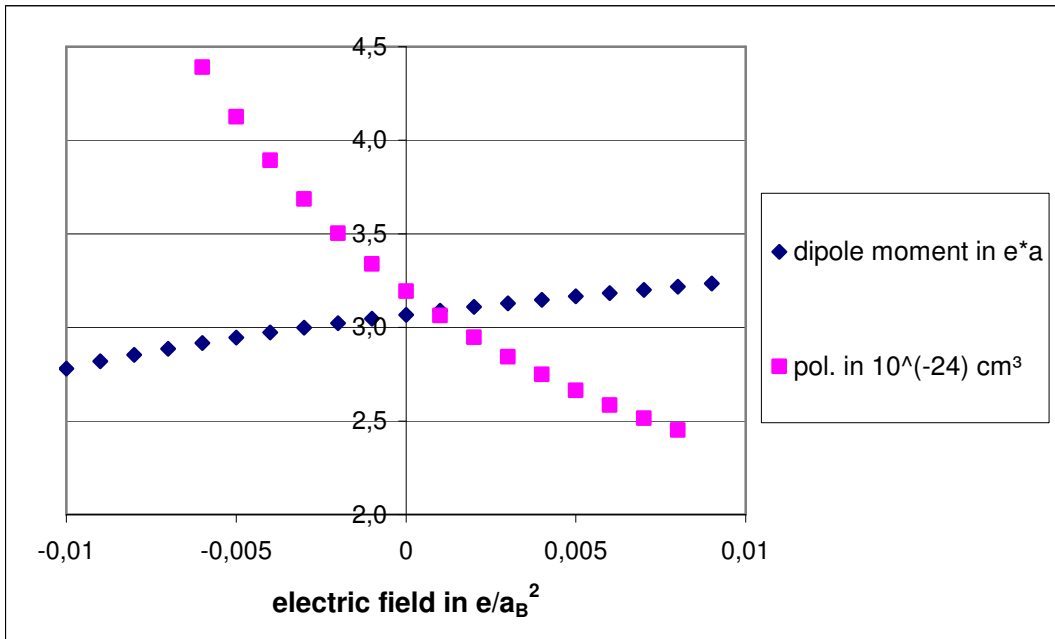
The second question we want to answer is concerned with the relation $\alpha_{\shortparallel} > \alpha_\perp$. What is the difference between those two cases? For the purpose of answering this, again the use

of the LCAO picture is helpful. In this model the important feature of the p-orbitals along the axis is that they form hybrids with the neighbouring s-orbitals. Namely we get the electron states $|\gamma-\rangle$ and $|\gamma+\rangle$. Also the $|Na,3p_x\rangle$ and other higher lying orbitals are hybridized. This means that the additional transition $\langle\gamma-|\mu|\gamma+\rangle$ exists along the axis. According to the previous assumption of orthogonality for the atomic orbitals of separate atoms, this transition should be zero. But we know that there will be some overlap in the region between the nuclei, which will give a non-vanishing contribution and has to be included. Furthermore the state $|\gamma+\rangle$ is the LUMO and this means that the energy difference is very small, which increases the polarizability from this transition.

Finally the third question is the comparison of formula (2.36) with a direct computation of α_{tot}. Speaking of a total polarizability only makes sense parallel to the molecular axis; therefore no distinguishing is necessary. Putting the results of (2.39) and Table 2.5 into (2.36) results in:

$$\alpha_{tot} = (3.33 + 0.84) \cdot 10^{-24}\, cm^3 = 4.17 \cdot 10^{-24}\, cm^3 \tag{2.47}$$

Consequently formula (3.36) gives the correct result. This is also an important check, as it is hard to stay in the linear region of the induced electronic dipole moments and get a shift of the nuclei at the same time. The reason is a very strong nonlinearity in the induced electronic dipole moment along the axis (see Figure 2.7).

By comparing Figure 2.7 to Figure 2.1 it is obvious that the nonlinearities here are much more important. Especially, it seems to be very easy to bring the molecule back to a state without dipole moment. All this makes it harder to get α_{tot}, since the nuclei only change position when the forces are sufficiently high. Because we are in the minimum, the external field cannot be too small, otherwise the nuclei would not move at all!

2.4 Larger clusters

We now ask which of the larger configurations are worth looking at. One main criterion is the usefulness of the results for getting information about how to parameterize quasi-classical models. In addition, there are aspects of structures that are interesting in their own. For example Na_2F_2, because other research groups already studied it and thus we are able to compare, or Na_4F_4 which has two different configurations (ring & cube) that are lying very close in energy. Furthermore the cube is highly symmetric, namely of the space group T_d, which enables us to easily analyse the vibrational modes and frequencies.

2.4.1 The dimer Na_2F_2

The ground state configuration of the Na_2F_2 cluster belongs to the D_{2h} symmetry group. As mentioned, the interesting aspect here is that other theoretical and also experimental results exist. Looking at the changes from the monomer, the most obvious effect is an elongated bond length. We get $d_{Na-F} = 3.96 a_B$ in the dimer, which is an increase of 7.3% compared to the monomer. Furthermore, the molecule is not square, but the two Na atoms are closer to each other than the two F atoms. Those two distances are:

$$d_{Na-Na} = 5.37 a_B \qquad d_{F-F} = 5.83 a_B \qquad (2.48)$$

This would exactly correspond to a picture where we assign effective radii to the ions: The Fluoride ion has a larger radius and therefore this species is further apart. For comparison and notation it is easier to cite the bond angle at the Sodium atom instead of those two additional distances (see Figure 2.8).

We now summarize our results on geometry and compare them with paper [20], where we find a discussion of the dimer and the monomer, including citations of experimental results. The authors used restricted Hartree-Fock (RHF) and Møller-Plesset perturbation theory (MP2) to perform their calculations.
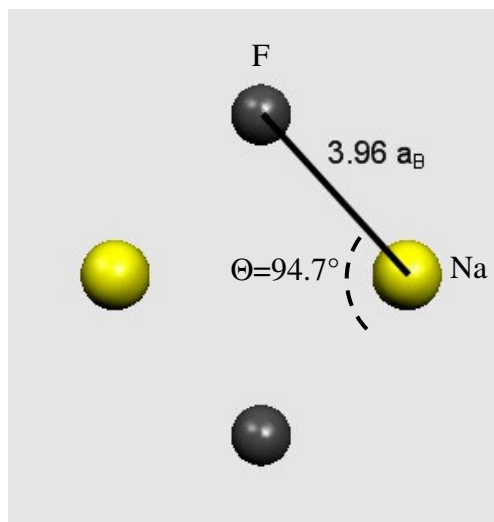
Fig. 2.8: Scheme of Na_2F_2

TABLE 2.8:
Comparing Na_2F_2 experiments with various theoretical results

	NRLmol	RHF [20]	MP2 [20]	Exp.1	Exp.2
Dimerization energy in eV	2.40	2.62	2.59	2.57 [27]	
d_{Na-F} in a_B	3.96	3.90	3.86	3.93(2) [28]	3.92(2) [29]
Θ in °	94.7	93.1	92.9	95.4(6) [28]	96.0(3.0) [29]

The dimerization energy can be obtained by taking the differences in the total energy of the dimer and twice the energy of the monomer.

$$E_{dim} = 2 \cdot E_{tot, NaF} - E_{tot, Na_2F_2} \qquad (2.49)$$

Since these numbers are very interesting for chemists and experimentally produced by them, they are often cited in kcal/mol instead of eV per formula unit. For convenience we cite the conversion factor:

$$1eV \; per \; formula \; unit = 23.05 \frac{kcal}{mol} \qquad (2.50)$$

Table 2.8 shows that our results for the geometry are of about the same quality as in the case of the monomer. Only the dimerization energy seems to be off by more than 5%, but then the experimental results are comparatively old and we have no information about the experimental error. Furthermore we observe that the RHF calculations also do pretty well and for this reason we want to compare our results for the vibrational frequencies with the RHF results from [20].

Since there are 12 degrees of freedom in this molecule, we get 6 vibrational frequencies with NRLmol. These frequencies are sorted according to the irreducible representation they belong to. Na_2F_2 is of the symmetry group D_{2h} which is of order 8 and has 8 classes. With this information and the use of the character table of this point group we can also get information about the geometrical shape of the vibrations and their IR and Raman activity.

TABLE 2.9: **Character table of the Na₂F₂ group D₂ₕ**

D_{2h}	E	C_2 (z)	C_2 (y)	C_2 (x)	i	σ(xy)	σ(xz)	σ(yz)		
A_g	+1	+1	+1	+1	+1	+1	+1	+1		x^2, y^2, z^2
B_{1g}	+1	+1	-1	-1	+1	+1	-1	-1	R_z	xy
B_{2g}	+1	-1	+1	-1	+1	-1	+1	-1	R_y	xz
B_{3g}	+1	-1	-1	+1	+1	-1	-1	+1	R_x	yz
A_u	+1	+1	+1	+1	-1	-1	-1	-1		
B_{1u}	+1	+1	-1	-1	-1	-1	+1	+1	z	
B_{2u}	+1	-1	+1	-1	-1	+1	-1	+1	y	
B_{3u}	+1	-1	-1	+1	-1	+1	+1	-1	x	
C_{12}	12	0	-2	-2	0	4	2	2		

The eight irreducible representations in Table 2.9 can be found with the help of the Great Orthogonality Theorem.

In addition, there are attached the characters of the representation of the molecule in Cartesian coordinates, which are labeled C_{12}. We use a 12-dimensional coordinate vector (Figure 2.9) and the corresponding matrices that perform the symmetry operations of this group. Thus we get the characters of our C_{12} representation. This representation can now be uniquely expressed as the sum of irreducible representations, because those are orthogonal. As result we obtain:

Fig. 2.9: Na_2F_2 12-D coordinates
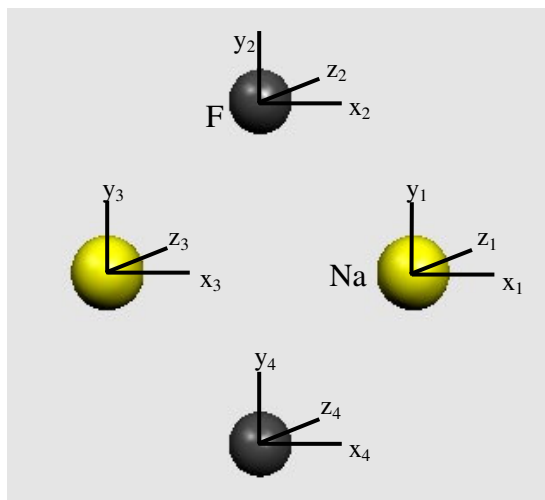
$$C_{12} = 2 \cdot \left(B_{1u} \oplus B_{2u} \oplus B_{3u} \right) \oplus 2A_g \oplus 2B_{1g} \oplus B_{2g} \oplus B_{3g} \tag{2.51}$$

If we now want to get the 6 representations for the vibrational modes, we have to subtract those which represent the translations and rotations. They are one set of the B_g for rotation and one set of B_u for translation. With this information we can assign the vibrational frequencies to the representations and compare them to the RHF results.

In addition there are also results by D. Welch computed with the classical 'shell model' (see subchapter 3.1) and experimental numbers for two of the IR-active modes. Furthermore we can find out the geometrical shape of those vibrations, since they are bases for their corresponding representation. We summarize the results in Table 2.10 and remind the reader, that the Sodium atoms are lying on the x-axis, whereas the z-axis is perpendicular to the molecular plane (see Fig. 2.9).
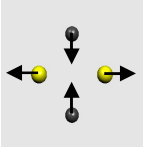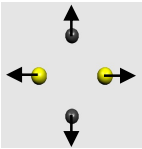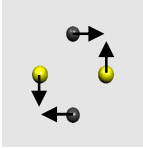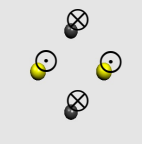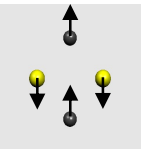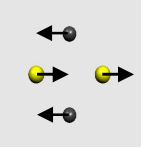
The RHF frequencies are always increased by 5.5- 8.5 % compared to NRLmol. Since this difference seems to be very systematic and already occurred in the monomer (see Table 2.5) and because correlation energy is not included in Hartree-Fock theory, part of this deviation might well be due to the neglection of correlation.

For the classical shell model, it can be observed that despite its comparatively simple form it captures most of the frequencies closely.

The only experimental check available is for the IR-active vibrations, where the results were obtained in absorption with the matrix isolation technique [30]. Due to a low-frequency limit of the spectrometer the out-of-plane vibration could not be detected. Nevertheless, the other two experimental frequencies show very good agreement with the DFT values and in the experimental results it is also observable that they have both about the same intensity. In the course of that experiment the monomer frequency was

determined to lie at 515 cm^{-1}. This result is also closer to the DFT result than the other experimental values we cited in Table 2.5.

TABLE 2.10: **Vibrational frequencies in cm^{-1} of the Na$_2$F$_2$ molecule**

	A_g	A_g	B_{1g}	B_{1u}	B_{2u}	B_{3u}
Shape						
Activity*	Raman (0.047)	Raman (1)	Raman (0.027)	IR (0.80)	IR (1)	IR (0.98)
NRLmol	205	377	326	149	373	362
RHF [20]	219	404	350	162	394	383
Shell model [31]	264	360	218	184	324	299
Exp.[30]				<190	380	363
RHF/ NRLmol	1.068	1.072	1.074	1.087	1.056	1.058

* The numbers in parenthesis relate the intensities. The highest intensities for IR and Raman respectively are set to 1.

We finish our study of the Na$_2$F$_2$ molecule with a discussion of the electronic and vibrational polarizability tensor.

$$\hat{\alpha}_e = \begin{pmatrix} 4.32 & & \\ & 3.75 & \\ & & 3.70 \end{pmatrix} \cdot 10^{-24}\, cm^3; \quad \hat{\alpha}_{vib} = \begin{pmatrix} 4.02 & & \\ & 3.84 & \\ & & 19.44 \end{pmatrix} \cdot 10^{-24}\, cm^3 \quad (2.52)$$

First of all we see that the electronic polarizability is far less than twice the value we get for the monomer. The second observation we make is that the anisotropy is also weaker than in the monomer. Since we know the crystal behaviour, which has isotropic α, we can already see that the smaller structures have a very special behaviour of α. There the direct influence of the interplay of atomic orbitals is still very present, which results in the anisotropies and unexpectedly large values for α_e. For the Na$_2$F$_2$ structure we therefore expect slightly larger static charges than in the monomer. This tendency should remain

valid as we go to bigger clusters and finally approach values of ±1. Furthermore the polarizability should become more and more isotropic while approaching the crystal value.

Especially the vibrational polarizability has increased very remarkably compared to the monomer. Namely the value along the z-direction is huge, which is partly explained by the low-frequency vibrational mode along this direction.

2.4.2 The Na$_4$F$_4$ cluster

We arrive at the last structure to which we will dedicate a separate subchapter, Na$_4$F$_4$. What makes it especially worthwhile to take a closer look at, is that there exist two different conformations which lie very close in energy, a cube and a ring. The separation in energy is so low, that the higher lying structure, the ring, will coexist at a small ratio even at room temperature. Our result for the energy difference is 0.75 eV, whereas another paper cites a value of 0.34 eV [32]. This paper studies the isomerization dynamics of those two different structures, where a factor of more than 2 in the energy differences is of course of exponential impact, since we look at statistical occupancy.

Both structures are highly symmetric, the cube belonging to the same symmetry group as methane, T$_d$. On the other hand the ring also has interesting symmetry properties, being of the group D$_{4h}$. Since we get a total of 18 different vibrational modes, this will make it easier to sort them out. Studying the geometry, we can see that the F nuclei in the cube are again further out from the center than the Na nuclei. Setting the center of mass as origin, we get:

$$Cube: \quad x_F = y_F = z_F = 2.12 a_B; \quad x_{Na} = 2.02 a_B \qquad (2.53)$$

Overall, the cube is very close to a fragment of the crystal, because the bond length is 4.33 a$_B$, compared to 4.37 a$_B$ for the crystal. In the ring the bond length is even shorter than in the dimer, since it has more of the features of a chain. The structures together with the geometric parameters are depicted in Figure 2.10.

Parallel to the dimerization energy of the last subchapter we can compute the "quadrimerization energy":

$$E_{quad} = 4 \cdot E_{tot, NaF} - E_{tot, Na_4F_4} = 7.10 eV \qquad (2.54)$$

Fig. 2.10: Comparing the cube and ring structure of Na_4F_4
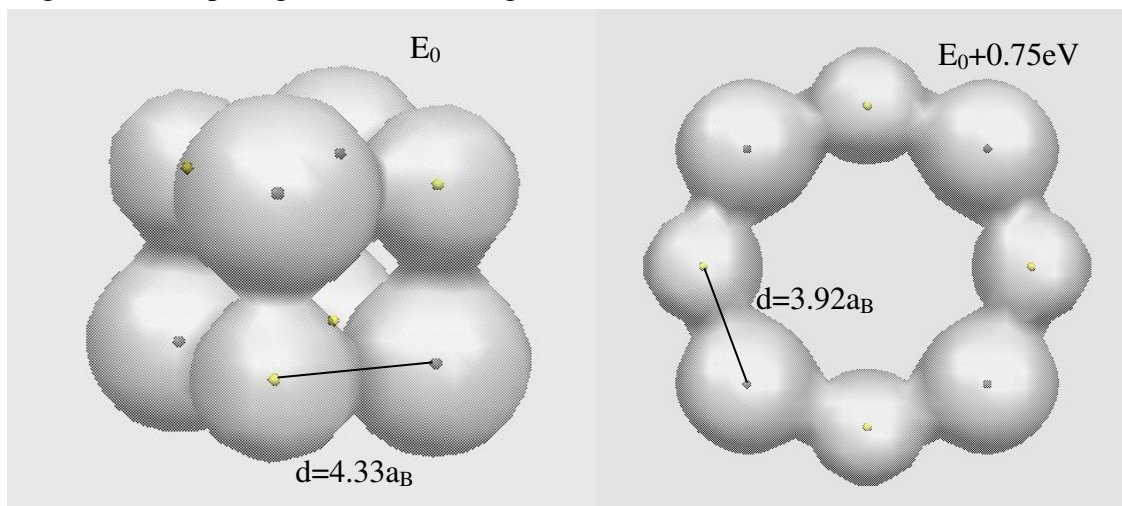
It is almost three times as big as the dimerization energy, which can be understood by visualizing the process in the following way: We start with four monomers and first form a dimer out of the first two, getting the dimerization energy. Next we attach the third monomer to the dimer, getting approximately the dimerization energy a second time (it will be a little bit less!). As a final step we form our cube and get our last energy gain, which explains why the quadrumerization energy is bigger by an approximate factor of 3.

Another interesting energy is the formation energy, which is the energy obtained per formula unit (per monomer), when making a cluster out of free atoms. In the present case it is just the dissociation energy of the monomer (2.38) plus one forth of the quadrumerization energy. This means that the formation energy will presumably increase with the size of the cluster until it reaches its maximum for the crystal structure (9.30 eV).

Consequently the biggest part can be gotten by forming the monomer, and later on the increases become smaller. For the cube the formation energy is 7.01 eV, which should be very close to the energy of a pair of corner atoms in the crystal.

Having discussed geometry and energies, it remains to take a look at the vibrational frequencies and the polarizabilites. Let us start with the vibrations of the cube. Using Cartesian coordinates parallel to the version in Fig. 2.9, we get a 24-dimensional vector. We label this representation as C_{24} and attach the characters at the end of the T_d character table.

TABLE 2.11: **Character table of the cube Na$_4$F$_4$ group T$_d$**

T$_d$	E	8 C$_3$	3 C$_2$	6 S$_4$	6 σ_d		
A$_1$	1	1	1	1	1		x^2+y^2+z^2
A$_2$	1	1	1	-1	-1		
E	2	-1	2	0	0		x^2-y^2, 2z^2-x^2-y^2
T$_1$	3	0	-1	1	-1	R$_x$, R$_y$, R$_z$	
T$_2$	3	0	-1	-1	1	x, y, z	xy, xz, yz
C$_{24}$	24	0	0	0	2		

As before we can split the C$_{24}$ representation into irreducible representations:

$$C_{24} = 2A_1 \oplus 2E \oplus 2T_1 \oplus 4T_2 \qquad (2.55)$$

Since one T$_1$ represents the rotations and one T$_2$ the translations, we know of which irreducible representations our vibrations will be. This also gives the information, that there exist a total of eight different frequencies, with a total of 18 modes. In principle we can now assign the geometrical shape to each vibrational frequency we calculated, as we did in Table 2.10 for the dimer. Nevertheless this task would be very tedious, especially because the T$_1$ and T$_2$ representations are more complicated.

Therefore we only summarize the frequencies and their activities in Table 2.12.

TABLE 2.12: **Vibrational frequencies of the Na$_4$F$_4$ cube**

| Frequency in cm^{-1}	151	159	250	253	262	305	313	317
# of modes	3	2	3	1	2	3	1	3
Irr. Representation	T$_2$	E	T$_1$	A$_1$	E	T$_2$	A$_1$	T$_2$
Activity*	IR (0.017) Raman (0.014)	Raman (0.007)	--	Raman (0.20)	Raman (0.028)	IR (0.18) Raman (0.002)	Raman (1)	IR (1) Raman (0.004)

* The numbers in parenthesis relate the intensities. The highest intensities for IR and Raman respectively are set to 1.

Apparently the vibrational frequencies have become lower in comparison to the dimer and especially to the monomer. If we compute the average of all frequencies weighed with their number of modes, we get the following result:

$$\bar{f}_{NaF} = 510cm^{-1}; \quad \bar{f}_{Na_2F_2} = 299cm^{-1}; \quad \bar{f}_{Na_4F_4} = 249cm^{-1} \qquad (2.56)$$

For comparison it is interesting to look at a 1-d model. We classically compute the vibrational frequencies of chains made of N atoms of one atomic species. They all have masses m and force constants k. We thus get (N-1) different frequencies for each chain. Denoting these frequencies as $f_N(1)$, …, $f_N(N-1)$ and their arithmetic average as f_N, we can re-express all the f_N as multiples of f_2. For N= 3,4 the results are very easy, and as going to infinity we get the phonon dispersion curve, which can be used to compute the average and therefore f_∞.

Fig. 2.11: Classical vibrations of 1-d chains
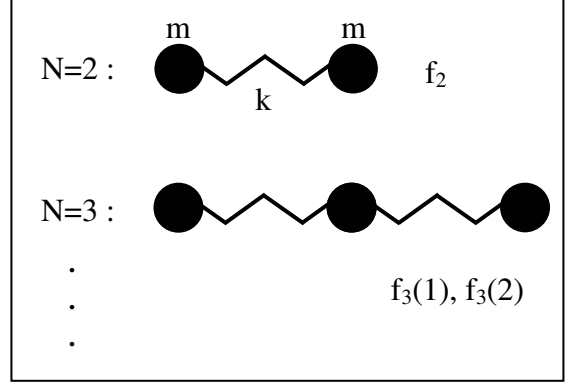
$$f_3 = \frac{1}{2}\left(\sqrt{\frac{1}{2}} + \sqrt{\frac{3}{2}}\right) \cdot f_2 \cong 0.966 \cdot f_2; \quad f_4 = 0.949 \cdot f_2; \quad …; \quad f_\infty = \sqrt{\frac{1}{2}} \cdot f_2 \qquad (2.57)$$

Now we do of course not deal with a 1-d chain of atoms of one species. Nevertheless the two atoms are very close in mass ($23m_0$ for Na and $19m_0$ for F), which implies that the splitting between the acoustical and optical branch in 1-d would be very small. This means that their average would be very close to $\sqrt{1/2}\, f_2$. Additionally we can also expect the average of the transverse branches in 3-d to be of the same size. On the basis of this model, we conclude that the force constant decreases in the larger structures, especially since the minimum of f_i occurs at f_∞. Otherwise a distinctly higher average of the vibrational frequencies would be expected.

There also exists a generalization of (2.36) for multi-particle systems (see formula 13 in [33]). This formula keeps all the essential features of (2.36) and this leads to the expectation of an increase in the vibrational polarizability.

$$\alpha_{vib,ij} = \sum_\kappa \frac{1}{\omega_\kappa^2}\left(\frac{\partial\mu_i}{\partial Q_\kappa}\right)\left(\frac{\partial\mu_j}{\partial Q_\kappa}\right) \qquad (2.58)$$

40

In (2.58) the sum goes over all vibrational modes (indexed with κ). The derivatives of the dipole moment components μ_i, μ_j are taken with respect to the normal mode coordinates of the vibrations.

Having studied the vibrations of the cube, we can do the same steps for the ring. The huge Character Table of the D_{4h} group can be found in [12]. By using again the C_{24} representation and getting its characters corresponding to the D_{4h} symmetry operations, we split it into the irreducible representations:

$$C_{24} = 4E_u \oplus 2E_g \oplus 2A_{1g} \oplus 2A_{2g} \oplus 2B_{1g} \oplus 2B_{2g} \oplus 2A_{2u} \oplus B_{1u} \oplus B_{2u} \qquad (2.59)$$

The translations are $A_{2u} \oplus E_u$ and the rotations $A_{2g} \oplus E_g$. This means we know the representations for all 18 vibrational modes. Important to note is that the $C_2{}'$ axis is identical to the x-axis and that the σ_v plane is perpendicular to the y-axis, i.e. they go through two Sodium atoms. The z-axis is perpendicular to the molecular plane.

TABLE 2.13: **Vibrational frequencies of the Na_4F_4 ring**

Frequency in cm^{-1}	30	40	41	49	97	99	141
# of modes	1	1	1	1	2	2	1
Irr. Re-presentation	B_{1g}	B_{2g}	B_{1u}	B_{2u}	E_g	E_u	A_{2u}
Activity*	Raman (0.011)	Raman (0.001)	--	--	Raman (0.002)	IR (0.37)	IR (0.99)
Frequency in cm^{-1}	160	221	281	385	392	460	471
# of modes	1	1	2	1	1	2	1
Irr. Re-presentation	A_{1g}	A_{1g}	E_u	B_{2g}	B_{1g}	E_u	A_{2g}
Activity*	Raman (0.036)	Raman (1)	IR (0.008)	Raman (0.061)	Raman (0.054)	IR (1)	--

* The numbers in parenthesis relate the intensities. The highest intensities for IR and Raman respectively are set to 1.

What distinguishes the ring frequencies from the cube is the broader range of values. Especially at the low energy end there are multiple vibrations in the ring, but none in the cube. This originates from the chain-like structure of the ring and the fact that vibrations can occur where the nuclei approach far less for some fixed amplitude than they would for any other vibration in the cube. Therefore the average frequency is even less, only

211 cm^{-1}. It is interesting to look at the two lowest lying vibrations. They both have the same geometrical shape, belonging to B_{1g} and B_{2g}. Only the two atomic species are exchanged. The lowest lying vibration is depicted in Figure 2.12, where we can see that the Sodium atoms move exactly along the axes and the Fluoride atoms at an angle of ~45°. If we move the Sodiums some distance d, the Fluorides move 0.39 d. Nevertheless, the neighbouring nuclei will only approach or go apart by 0.047 d. This means that the effective force constant is reduced by a remarkable factor, and that explains the very low frequency of this vibrational mode.

Fig. 2.12: Na$_4$F$_4$ ring vibration with f = 30cm^{-1}
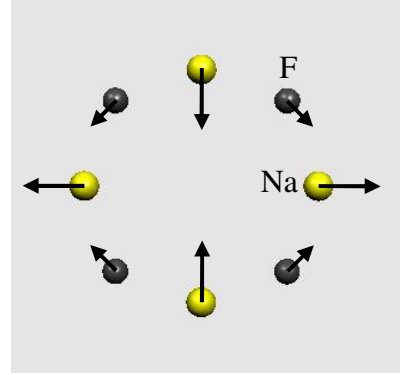
Finally we present the electronic polarizabilities. For the cube it is a scalar and for the ring only the polarizability along the z-axis is different.

$$\hat{\alpha}_{e,cube} = 6.95\,\hat{E} \cdot 10^{-24}\,cm^3; \quad \hat{\alpha}_{e,ring} = \begin{pmatrix} 7.87 & & \\ & 7.87 & \\ & & 6.97 \end{pmatrix} \cdot 10^{-24}\,cm^3 \qquad (2.60)$$

In the ring the polarizability is lowest out of the molecular plane. That was already the case in the dimer and also in the monomer, where the polarizability perpendicular to the axis was lower due to additional transitions along the axis. Overall we can see the tendency that the polarizability per NaF pair decreases. To get some check for our notion, we computed one of the octupole moments for the cube and formally assigned a static charge q according to it. Since the x,y,z coordinates of the nuclei of one species all have the same absolute value, we make the approach:

$$\int d^3r\, x\,y\,z\,\rho(\vec{r}) = 4q\,x_{Na}^3 + 4q\,x_F^3 \quad \rightarrow \quad q = \frac{\int d^3r\, x\,y\,z\,\rho(\vec{r})}{4x_{Na}^3 + 4x_F^3} \qquad (2.61)$$

In this formula ρ denotes the total charge density, i.e. electron density + point charges of the nuclei. As result a formal static charge of q = 0.866 e is computed, compared to the static charge of 0.831 e in the monomer. This would correspond to a weaker contribution of the |Na,3s⟩ atomic orbitals and therefore result in a decreased total polarizability.

The next step is to take a look at the vibrational polarizability. As already expected on grounds of the decreased vibrational frequencies, there is a big enhancement compared to the monomer. For the cube α_{vib} is isotropic and therefore only a scalar.

In the monomer we had one vibration along the axis. If we only look at this direction, we therefore had one mode per NaF pair. In the Na$_4$F$_4$ cube we have 18 vibrations for 3 directions of space. This leads to the expectation of an enhancement factor of 6 for the

vibrational polarizability. In addition, the average of our vibrational frequencies was only about half that of the monomer, while the force constant stands in the denominator. This implies another increase, especially as low frequency vibrations create very large contributions.

The result of the calculation agrees with our expectation.

$$\alpha_{vib,cube} = 10.35 \cdot 10^{-24} \, cm^3 \tag{2.62}$$

Taking a look at the ring structure, we expect a different result. On grounds of the result for the dimer we again predict a large value of α_{vib} out of the molecular plane.

$$\hat{\alpha}_{vib,ring} = \begin{pmatrix} 36.01 & & \\ & 36.01 & \\ & & 41.28 \end{pmatrix} \cdot 10^{-24} \, cm^3 \tag{2.63}$$

The value out of the plane is indeed about twice that of the dimer, but additionally we also get comparably large results in the plane. Going back to our two lowest frequencies we see that they both are in the molecular plane. This provides an explanation for the result.

With the anisotropy becoming less and especially as it is desirable for classical models to have isotropic polarizability assigned to all components of a cluster, it also makes sense to look at the average value. Additionally this might be more useful for comparison with experiment.

Another interesting result, especially for comparison with classical models, is the induced quadrupole moment in the cube configuration. The definition of the electronic quadrupole tensor elements can be found in [34], where Buckingham discusses intermolecular forces.

$$\Theta_{\alpha\beta} = \frac{1}{2} \sum_i q_i \left(3 r_\alpha^i r_\beta^i - \vec{r}^2 \delta_{\alpha\beta} \right) \tag{2.64}$$

When applying an external field perpendicular to one side of the cube, assigning the field in z-direction, we get an induced quadrupole moment in xy-direction.

$$\Theta_{xy} = \frac{3}{2} \int d^3 r \, x \, y \, \rho(\vec{r}) \tag{2.65}$$

This induced quadrupole moment can also be computed with other models and therefore provides a valuable check. Now we make calculations and express Θ_{xy} as a function of the external field in z-direction $\Theta_{xy}(F_z)$. For zero field this expression vanishes because of the symmetry properties of the tetrahedron. For small fields there is a linear relation.

Fig. 2.13: Induced quadrupole moment in the Na_4F_4 cube

F-field in atomic units

$y = -8{,}1998x + 0{,}0002$
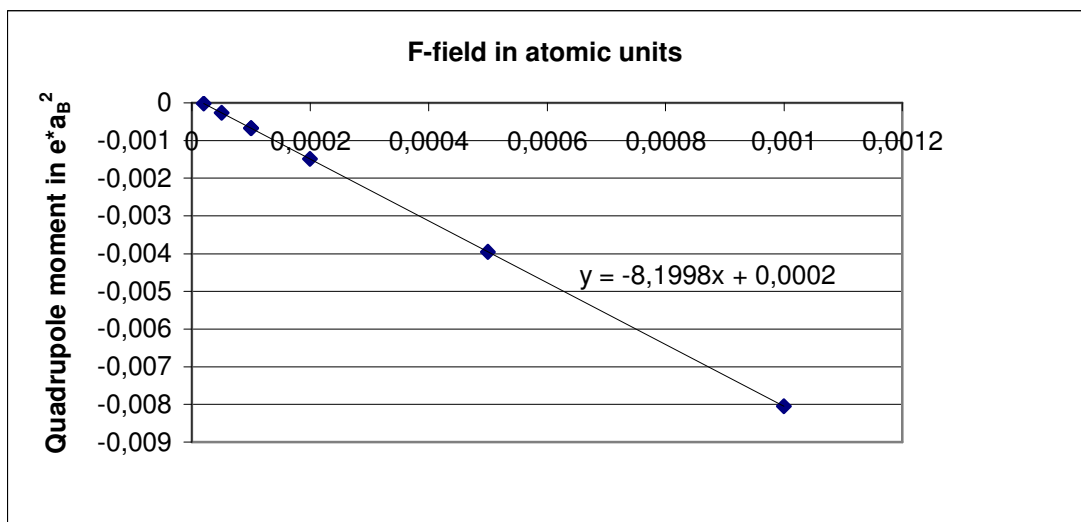
From the linear fit in Figure 2.13 we get the quadrupole polarizability.

$$\Theta_{xy}(F_z) = \left(-8.2\,a_B^4\right) \cdot F_z \tag{2.66}$$

2.4.3 Clusters with more than 10 atoms

This last part of chapter two presents the results on bigger clusters, where no experimental results are available. In some cases there exist at least other theoretical studies, which will be used for comparison.

Na_6F_6

This structure of D_{2h} symmetry is the next biggest crystal fragment after Na_4F_4 and has no net dipole moment. The bond length between the inner four atoms is distinctly longer than on the outer ones. This will be a general

Fig. 2.14: Na_6F_6 geometry with distances in a_B
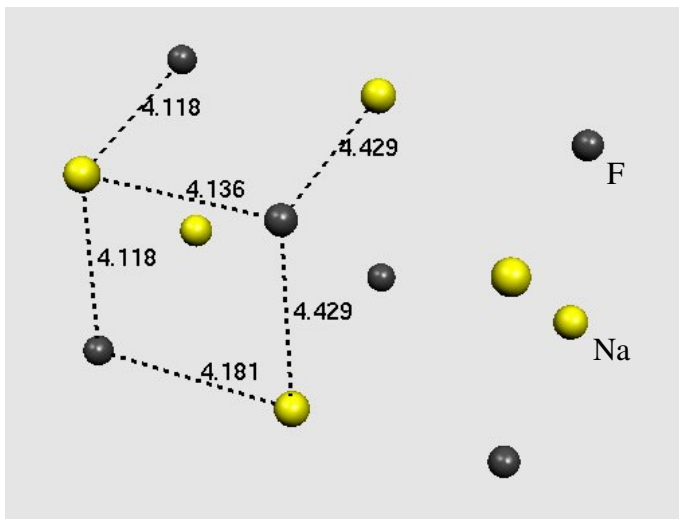
phenomenon in all clusters. The corner atoms are always slightly impressed towards the center of the cluster. We also computed the formation energy of that cluster.

$$E_{form}(Na_6F_6) = 7.18eV \qquad (2.67)$$

This is only slightly higher than the result for the Na_4F_4 cube, but when we consider that the formation energy of the corner atom pairs should be approximately the same, the formation energy of the inner (or edge) pairs is calculated to 7.53 eV, which is already much closer to the crystal value.
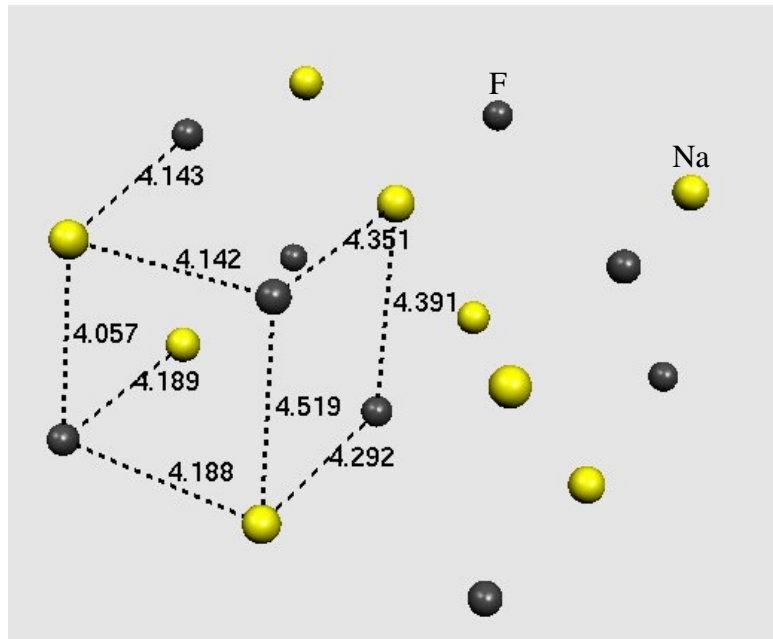
Na₉F₉

Fig. 2.15: Na₉F₉ geometry (3x3x2) with distances in a_B

Consisting of 18 atoms and being of C4v symmetry, this cluster has a dipole moment perpendicular to its 3x3 plane, because of the uneven number of ions in each plane.

$$\mu = 2.01 \text{ e a}_B \qquad (2.68)$$

This dipole moment is only about half that of a point-charge model with charges of ±e, implying that the ionization is not total. In addition the expected rise in the formation energy compared to Na₆F₆ can be confirmed.

$$E_{form}(Na_9F_9) = 7.31eV \qquad (2.68)$$

In combination with the results for Na_4F_4 and Na_6F_6 this provides a basic estimate for the energy of a pair of face atoms to 7.63 eV.

We also calculated the polarizability tensors of the Na₉F₉ cluster.

$$\hat{\alpha}_e = \begin{pmatrix} 15.1 & & \\ & 15.1 & \\ & & 14.2 \end{pmatrix} \cdot 10^{-24}\, cm^3\,; \quad \hat{\alpha}_{vib} = \begin{pmatrix} 29.1 & & \\ & 29.1 & \\ & & 28.7 \end{pmatrix} \cdot 10^{-24}\, cm^3 \quad (2.69)$$

The last component in both tensors is the one perpendicular to the 3x3 plane. Compared to the Na_4F_4 cube, the ratio α_{vib}/α_e is considerably increased and it would be interesting to find out at what cluster size this ratio will reach the bulk limit. For the bulk the dielectric constants are ε_∞= 1.7 and ε_0= 5.1 [35]. Comparing those numbers to the bulk limit of the polarizabilities would be an interesting topic for further research.

Instead of listing all the vibrational frequencies, we plot them together with their infrared intensities in Figure 2.16.

Fig. 2.16: Vibrational frequencies of Na_9F_9. Each single mode is plotted as a diamond and the diamonds are connected to show the IR-spectrum
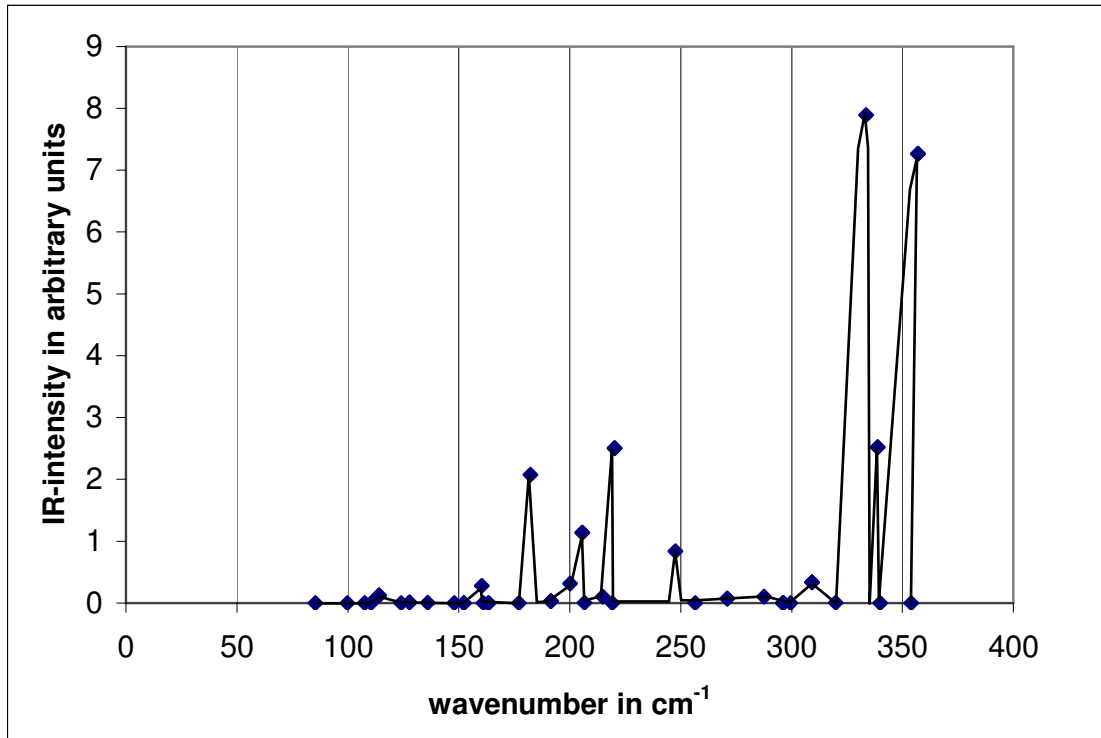
$Na_{14}F_{13}$

Due to its interesting symmetry properties, this cluster has already been investigated in the literature. Rayane *et al.* studied a broad range of clusters with configuration Na_nF_{n-1} and experimentally determined their dipoles and polarizabilities [36].

In addition, they theoretically modelled them as consisting of ions, for which pseudo potentials are used, and one excess electron which is treated quantum mechanically.

With this simple model they found a breaking of the O_h symmetry in $Na_{14}F_{13}$ due to a second-order Jahn-Teller effect. This means they computed a ground state of C_{3v} symmetry along the (111)-axis, with a big dipole in this direction. Despite that big dipole the energy difference of this structure and O_h was calculated to only 0.04 eV, which is of course far smaller than

Fig. 2.17: $Na_{14}F_{13}$ geometry (3x3x3) with distances in a_B

the error in their calculation. Furthermore they also find electron states centered on one of the edges (C_{2v}) or faces (C_{3v}) (with the corresponding nuclear distortions) which are lower by 0.02 eV and 0.01 eV compared to O_h symmetry. Accordingly, their symmetry breaking is a ferroelectric instability, because it spontaneously creates a big dipole.

Since effects of this type have already been predicted by Landman *et al.* in 1985 for Sodium Chloride [37], and later on studied by Ochsenfeld *et al.* for $K_{14}Cl_{13}$ and $Li_{14}F_{13}$ [38], it seems reasonable to take these effects as real. On the other hand Ochsenfeld *et al.* predict the effect for $Li_{14}F_{13}$ to be much smaller than in clusters where heavier Halides are used. Since the ionic polarizability of Fluoride is considerably lower than those of other Halides, a ferroelectric instability seems to be less likely.

For this reason we use our more accurate NRLmol code to calculate the vibrational spectrum and see whether there exist negative frequencies corresponding to a saddle point in the energy surface and having as consequence a symmetry breaking. However, our calculation does not confirm this notion; instead we find a normal spectrum comparable to the ones we calculated for other clusters.
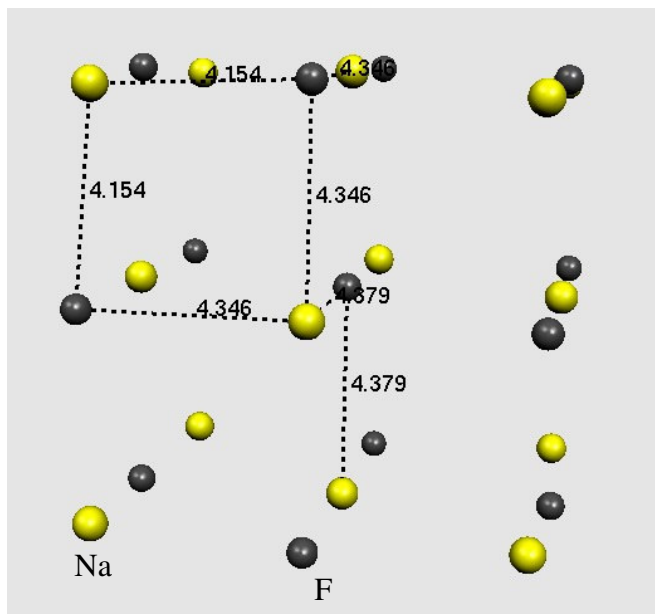
Fig. 2.18: Vibrational frequencies of $Na_{14}F_{13}$. Each single mode is plotted as a diamond
and the diamonds are connected to show the IR-spectrum

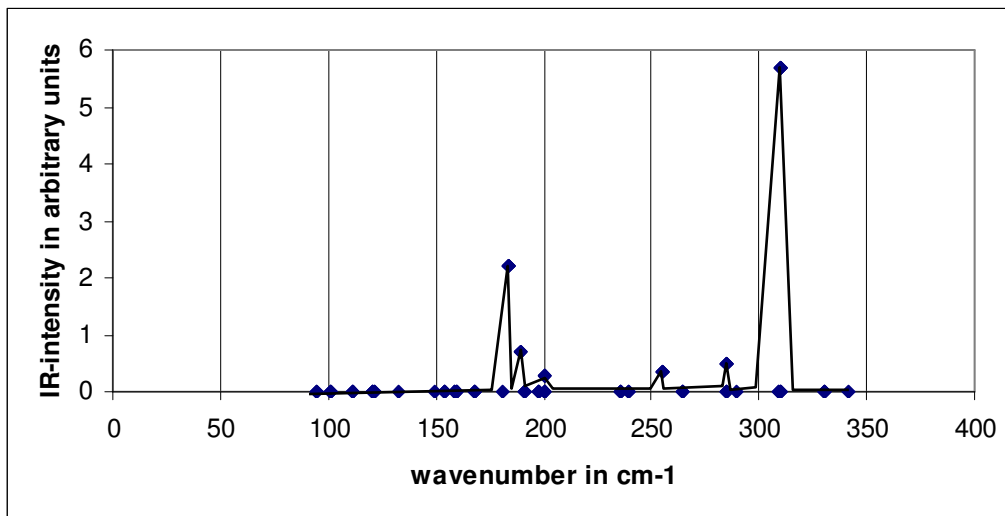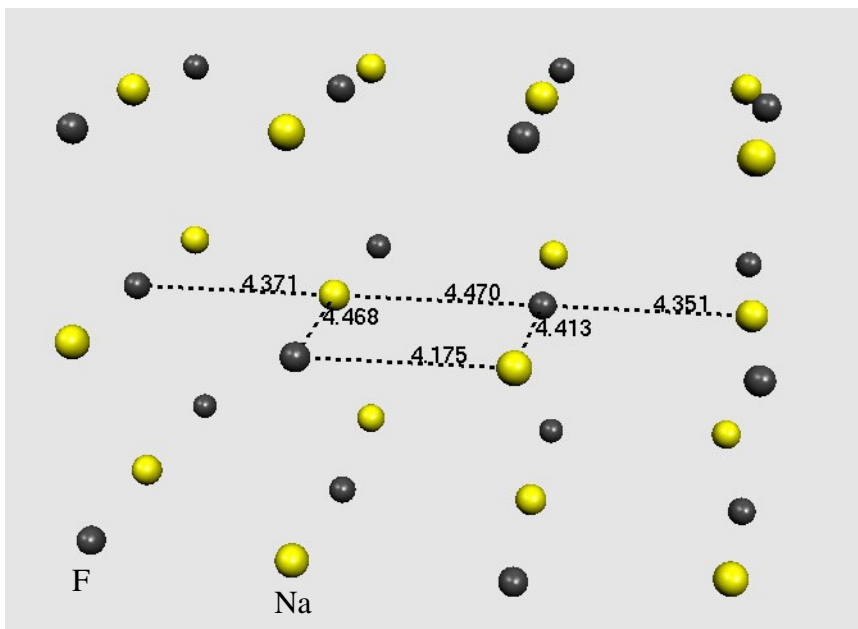Fig. 2.19: $Na_{18}F_{18}$ (4x3x3) with distances in a_B

Na$_{18}$F$_{18}$

We chose this cluster as the last one to compute, because it is the first structure where a
NaF pair is totally surrounded by other ions. Furthermore this structure has a dipole

moment along the z-axis, where four ions occur in a row. This dipole moment can be compared to the $Na_{18}F_{17}$ cluster, where one Fluoride corner atom is missing.

$$\vec{\mu}(Na_{18}F_{18}) = \begin{pmatrix} 0 \\ 0 \\ 5.12 \end{pmatrix} e\,a_B \; ; \quad \vec{\mu}(Na_{18}F_{17}) = \begin{pmatrix} 0.38 \\ 0.38 \\ 4.57 \end{pmatrix} e\,a_B \qquad (2.70)$$

Apparently, the missing ion is replaced by a surface state of the highest lying electron, which partly compensates the effect so that the dipole moment is only slightly changed. In [36] the dipole moment of $Na_{18}F_{17}$ was computed to 5.08 e a_B and thus lying close to our result of 4.60 e a_B.

Next it is interesting to look at the formation energy.

$$E_{form}(Na_{18}F_{18}) = 7.53\,eV \qquad (2.71)$$

This is especially interesting, since this calculation together with the formation energies of Na_4F_4, Na_6F_6 and Na_9F_9 are sufficient to estimate all the energies of NaF pairs occurring in the crystal. For corner, edge and face atoms this was already done during the previous calculations, but now we can summarize all four estimates.

TABLE 2.14:
Estimates of the energies of bulk corner, edge, face and center NaF pairs in eV

corner	edge	face	center
7.01	7.53	7.63	9.11

Even if this estimate can only be considered as rather crude, the result for the center pair is very close to the experimental bulk value of 9.30 eV. Furthermore, a refinement of our result can simply be done by additional calculations on larger NaF-clusters.

Before finishing our DFT studies with the IR-spectrum of this cluster, we present the two polarizability tensors.

$$\hat{\alpha}_e = \begin{pmatrix} 28.2 & & \\ & 28.2 & \\ & & 29.8 \end{pmatrix} \cdot 10^{-24}\,cm^3 \; ; \quad \hat{\alpha}_{vib} = \begin{pmatrix} 52.8 & & \\ & 52.8 & \\ & & 62.7 \end{pmatrix} \cdot 10^{-24}\,cm^3 \quad (2.72)$$

Compared to Na_9F_9 the ratio α_{vib}/α_e remains practically unchanged, which increases the interest whether this remains valid for even larger clusters.

Finally we plot the vibrational frequencies and their predicted IR-spectrum.

Fig. 2.20: Vibrational frequencies of $Na_{18}F_{18}$. Each single mode is plotted as a diamond
and the diamonds are connected to show the IR-spectrum
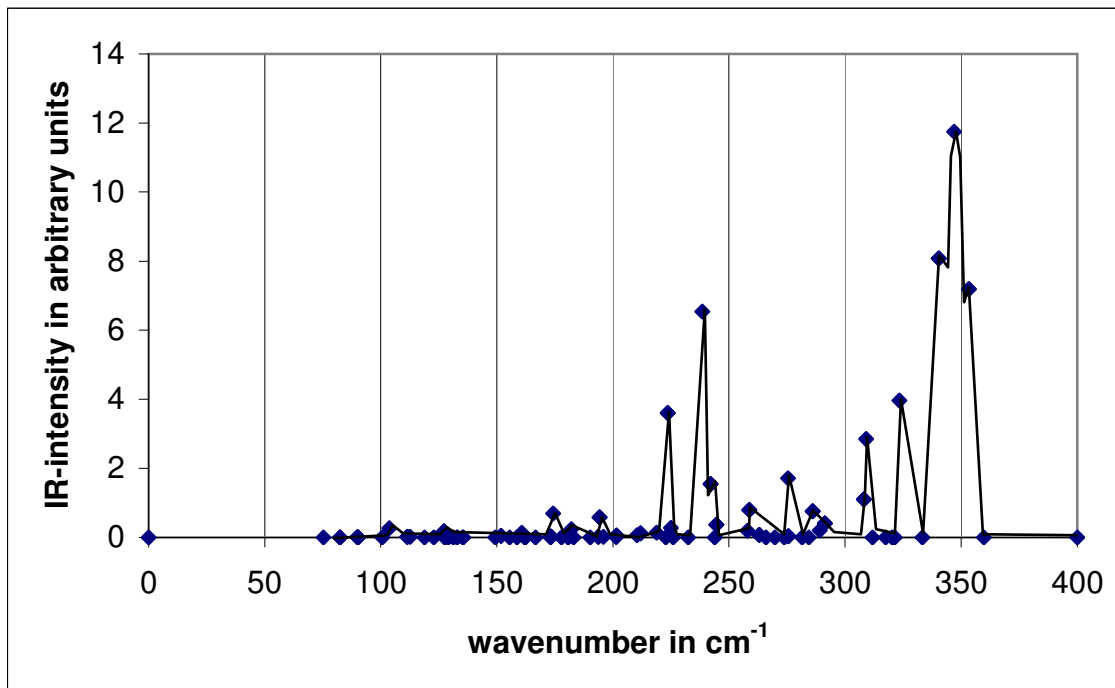
The spectrum resembles the Na_9F_9 spectrum closely. Both have the high IR-active peaks
at $\sim$340 cm^{-1}.

Chapter 3

Classical models

3.1 Motivation

After spending most part of this thesis for DFT calculations and the discussion of the results in the scheme of quantum mechanics, let us take one step back and think about classical mechanics models. Subchapter 1.3 already gave a brief discussion, and the question is why it might be advantageous to have classical models in addition to such powerful theories as DFT.

   To clarify this point, we summarize the development of models that describe systems using classical mechanics. We confine ourselves to ionic compounds, where the alkali halides present the most important subgroup. For these crystals the important feature, as the name implies, is that the atoms are practically ionized. Unlike covalent bonding (which is quantum mechanical) there is an obvious classical contribution to the energy: The Coulomb energy of the ions.

   This energy alone already accounts for crystal formation. It is a simple theoretical problem and can easily be obtained from experiments that the energy cost for ionization of the cations minus the electron affinity of the anions will be regained at a distance considerably bigger than the crystal bond length. Consequently, in the simplest model, we only need one additional energy term that stops the ions at the equilibrium bond length and prevents them from falling into each other. As is known from quantum mechanics this repulsion results from the overlap of the electron shells and therefore it is most realistic if it decreases rapidly at larger distances. Accordingly, the obvious choice is the so-called Born-Mayer repulsive energy term, used in many classical models, sometimes in slight variations.

$$E_{BM} = A_{ij} \cdot \exp\left(-\lambda_{ij} \mid \vec{r}_{ij} \mid\right) \tag{3.1}$$

In formula (3.1) the two empirical parameters A_{ij} and λ_{ij} are both positive and obtained by fitting the model to crystal and/or molecular data.

Here we find the first difference between the original motivation and the current situation. In the past, the available computational power was not sufficient to get reasonably good *ab initio* results to which these parameters could be fit. Therefore the method of choice was to fit them to experimental data in order to have a model to predict other structures and properties. A fit to crystal data, which was widely used, is the one by Tosi and Fumi, dating back to 1964 [39]. From a theoretical point of view, this is not totally satisfying. It would be more interesting and consistent to make fits to *ab initio* data and compare the results with experiment after that.

This fit is quite good for the crystal structure, but as we go to smaller clusters the discrepancies become more and more obvious. Especially when looking at other properties, apart from energies and geometries, a less simplistic model is needed.

One improved model was developed and thoroughly tested by D. Welch *et al.* [31,40]. Their so-called "shell model" assigns fixed polarizabilities to each single ion and includes the electrostatic interaction energy of the induced dipoles. Important to note is that the ions are assumed point-polarizable, which means that the induced dipoles are exactly situated at the sites of the nuclei. Furthermore, a modification of the Born-Mayer repulsion is implemented to avoid a polarization catastrophe, i.e. a "valley" in the energy surface due to negative dipole-dipole interaction energy, leading to the global minimum of the total energy at zero bond length. In the Welch shell model the interaction energy of two ions is:

$$E(\vec{r}_{ij}) = \frac{Z_i Z_j e^2}{|\vec{r}_{ij}|} + A_{ij} \cdot \exp\left(-\lambda_{ij}\left|\vec{r}_{ij} + \frac{\vec{\mu}_i}{Q_i} - \frac{\vec{\mu}_j}{Q_j}\right|\right) + \frac{(\vec{\mu}_i \circ \vec{r}_{ij})Z_j e - (\vec{\mu}_j \circ \vec{r}_{ij})Z_i e}{|\vec{r}_{ij}|^3}$$

$$+ \frac{\vec{\mu}_i \circ \vec{\mu}_j}{|\vec{r}_{ij}|^3} - 3\frac{(\vec{\mu}_i \circ \vec{r}_{ij})(\vec{\mu}_j \circ \vec{r}_{ij})}{|\vec{r}_{ij}|^5} + \frac{|\vec{\mu}_i|^2}{2\alpha_i} + \frac{|\vec{\mu}_j|^2}{2\alpha_j} \qquad (3.2)$$

With this formula two additional empirical parameters are introduced: Q_i and the polarizabilities α_i. The energy terms are explained as follows:

After the Coulomb interaction of the ions we get the modified Born-Mayer energy. It can be visualized by imagining the repulsion to occur between the electron clouds, which are uniformly detached from the ions because of the induced dipoles. Next comes the Coulomb interaction between ions and dipoles. Finally we have the dipole-dipole interaction and the positive formation energy of the dipoles $\mu^2/2\alpha$.

Using this model Welch *et al.* computed vibrational frequencies, geometric parameters and various other values for a broad range of alkali halides.

At this point another reason for using classical models becomes obvious. It is due to the conflict between exactness and computer time. Single structure calculations might not

be the problem nowadays, but to make molecular dynamics simulations, the time factor becomes important again. Needing time steps of femtoseconds it is evident that a huge number of calculations are required to reach time spans where interesting things like structure conversions will happen.

Consequently, according to the problem one wants to solve, it has to be estimated which model will best serve the purpose. For static calculations *ab initio* methods present the first choice, but the more time steps required, the simpler the model has to be.

Therefore let us discuss one recent example where the application of the Welch model is sufficient and also necessary, because more complicated models and especially *ab initio* calculations would consume too much computer time. It is about an experiment on structural transitions of singly charged Sodium-Chloride clusters of the type $(NaCl)_n Cl^-$ [41]. R. Hudgins *et al.* found experimental evidence that some of the structures, which were produced by laser vaporization of a NaCl rod, decayed into a different geometrical conformation with the same number of atoms. As example, immediately after the vaporisation, there were 3 different structures of type $(NaCl)_{35}Cl^-$ (with the bulk fragment forms 5x5x3, 5x4x4 and 8x3x3). Depending exponentially on temperature, two of those structures had decayed into the third one after a certain time span. To explain these processes and the observed time spans, two other papers [42,43] (written by J. Doye and D. Wales) applied the Welch model to compute the energies of those structures and additionally the energies along the reaction pathways. To do this, they had to scan the potential energy surface as a function of the atomic coordinates, which involves a huge number of calculations. Thus *ab initio* methods are not practical. Then they set up a master equation for the transformations. The solution indeed was able to explain the processes. Even the observed half-lives of the different structures were reproduced very closely.

Apart from the approach by Welch *et al.* there exist many different other models, which can be crudely separated into two groups. First, there is the group which stays in the classical regime, but introduces more and more energy terms to model the various aspects of the systems. An example would be the work by P. Madden *et al.*, who among other things developed classical models for MgO [44-46]. The second group includes models where *ab initio* methods are incorporated and applied together with classical ideas. This seems to be especially promising in the field of molecular dynamics, since computer speed increases steadily and *ab initio* methods are superior to empirical classical models, when only the accuracy is compared.

However, going back to our motivation in 1.3, the main objective was to get intuitive insight, which can only be provided by models that are also simple enough to keep track of. This condition would be fulfilled by a model comparable to the Welch-model, but it would be preferable if the appearance of the dipoles could be avoided in the exponential Born-Mayer function. If the polarization catastrophe can be cured by other means, the

dipoles retain their classical behaviour. This would definitely be preferable for our purposes.

3.2 Application to NaF-clusters

3.2.1 Point-polarizable model for the NaF monomer

As in chapter 2, we start with the simplest system. What we learned about the monomer from DFT, was that the polarizability cannot simply be understood as the sum of the free ion polarizabilities. Nevertheless, those are commonly used in classical models, so it will be worthwhile to find out how far we can get with this model in the monomer.

Therefore we look at the molecule at fixed bond length d (simply the DFT result) and only worry about the dipole moment and the electronic polarizability. For this purpose fixed static charges ±q and polarizabilities α_{Na} and α_F are assigned to the ions.

Fig. 3.1: Scheme for the NaF monomer

The ionic dipoles will then optimize, in order that electric field and induced dipoles are consistent. In the course of this calculation all dipoles are counted positive when they point along th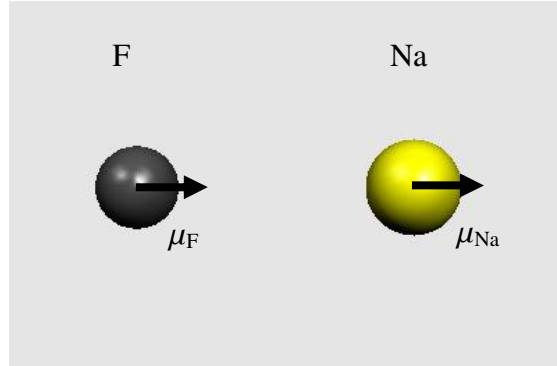e direction of the arrows in Figure 3.1. Last but not least we include the possibility of an external electric field, which is also counted positive parallel to the arrows.

The following equations are set up for the two dipole moments:

$$\mu_{Na} = \alpha_{Na}\left(-\frac{q}{d^2} + \frac{2}{d^2}\mu_F + F_{ext}\right); \quad \mu_F = \alpha_F\left(-\frac{q}{d^2} + \frac{2}{d^2}\mu_{Na} + F_{ext}\right) \tag{3.3}$$

Since they are totally symmetric, we also get symmetric solutions.

$$\mu_{Na} = \alpha_{Na} \frac{1 + \frac{2}{d^3}\alpha_F}{1 - \frac{4}{d^6}\alpha_F\alpha_{Na}}\left(-\frac{q}{d^2} + F_{ext}\right); \quad \mu_F = \alpha_F \frac{1 + \frac{2}{d^3}\alpha_{Na}}{1 - \frac{4}{d^6}\alpha_F\alpha_{Na}}\left(-\frac{q}{d^2} + F_{ext}\right) \quad (3.4)$$

Obviously, the polarizability of the ions is modified from the originally assigned value by the expression in front the parentheses. However, this "local field" enhancement is weak, because the cube of the bond length is far bigger than the polarizabilities. When we use the DFT results from Table 2.3 of $\alpha_{Na}= 0.14 \ 10^{-24} \ cm^3$ and $\alpha_F= 1.23 \ 10^{-24} \ cm^3$, the bond length d= $3.69a_B$ and q= 1, we get increases in the polarizabilities of 5.1% for α_F and 35% for α_{Na}. α_{Na} is small anyway, so this enhancement does not lead to a significant contribution.

By using (3.4) we can also set up the total dipole moment of the molecule and the total electronic polarizability.

$$\mu_{tot} = q \cdot d + \frac{\alpha_{Na} + \alpha_F + \frac{4}{d^3}\alpha_F\alpha_{Na}}{1 - \frac{4}{d^6}\alpha_F\alpha_{Na}}\left(-\frac{q}{d^2} + F_{ext}\right); \quad \alpha_{tot} = \frac{\alpha_{Na} + \alpha_F + \frac{4}{d^3}\alpha_F\alpha_{Na}}{1 - \frac{4}{d^6}\alpha_F\alpha_{Na}} \quad (3.5)$$

This result was also derived in [47]. By using the DFT numbers as input and setting $F_{ext}= 0$, we get for NaF:

$$\mu_{tot} = 2.96 \ ea_B ; \quad \alpha_{tot} = 1.48 \cdot 10^{-24} \ cm^3 \quad (3.6)$$

It can be seen that the total dipole moment is quite close to the DFT result, whereas the polarizability is far less than the DFT value of α_{tot}=3.33 $10^{-24} \ cm^3$. To amend the error in α_{tot}, there are two points which became clear during the studies of chapter 2. First we saw in 2.2.3 that the induced dipole moment cannot always be treated as linear in the applied field, namely we found an increase in the polarizability defined by (2.11) as we go to higher fields. Second, chapter 2.3.3 showed that the polarizability strongly depends on the charge of the ion. Both these insights seem to show that it is justified to improve the classical model by increasing α_{Na} and α_F.

Nevertheless, we find ourselves in a dilemma, since if we simply increase the polarizabilities used as input, the result for the total dipole moment moves further away from the DFT number. This implies that the second parameter q has to be changed. If we want to reproduce both the DFT polarizability and dipole moment, then we get the unacceptable result of q= 1.51 when fitting (3.5). By analysing (3.5) it becomes obvious that the fitting of the dipole moment is incompatible with the total polarizability. It is not

possible to satisfy both criteria and the result of the classical model will always be quite far off the DFT numbers.

Since for classical models polarizability and dipole moment have to be treated the way we did it, there seems to be no solution to satisfactorily reproduce the parameters of the monomer by only using the free ionic and atomic results plus a classical model.

3.2.2 Classical models for other structures

Since classical models have indisputable value, it seems wisest to acknowledge that they will not explain everything. In particular, diatomic NaF cannot be easily modelled with a classical story based on the free ions. Now we want to present a few ideas, where classical models might at least be applied to explain some of the phenomena found in chapter 2.

One of the outcomes of the DFT studies was that α_e strongly depends on structure and size of the molecule. This is hard to incorporate in classical models, but the way suggested by the DFT result would definitely be to have varying charges on the ions and to let the polarizabilities depend on those charges.

Another nice effect to investigate occurs in the Na_4F_4 cube. In a classical point-polarizable model we will get an induced quadrupole moment when applying an electric field along one of the C_2 axes. The interesting part is that the polarizability along this axis will not be enhanced the way we found it in 3.2.1. Namely, when applying an F-field in z-direction, the field created at ion site i will have in first order no induced component in z-direction apart from the external one. All fields created by the other induced dipoles will cancel exactly along the z-direction. Thus, apart from very small second-order effects, α_e of the point-polarizable ions can be obtained by fitting to the DFT result and then we can use the classical model to predict the quadrupole polarizability and compare to DFT.

For the classical calculation we assume perfect cubic symmetry with d= $4.33a_B$ (the DFT result). Then the second order induced dipoles are lying exactly in the xy-plane, all at angles of 90˚ to their neighbours. Since the directions are shown in Figure 3.2, we only use the absolute values of the dipoles in our calculations. The first order dipoles are directly induced by the external field in z-direction.

$$\mu_{Na}^{(1)} = \alpha_{Na} F_{ext} \; ; \quad \mu_F^{(1)} = \alpha_F F_{ext} \tag{3.7}$$

Fig. 3.2: First and second order induced dipole moments in the Na$_4$F$_4$ cube
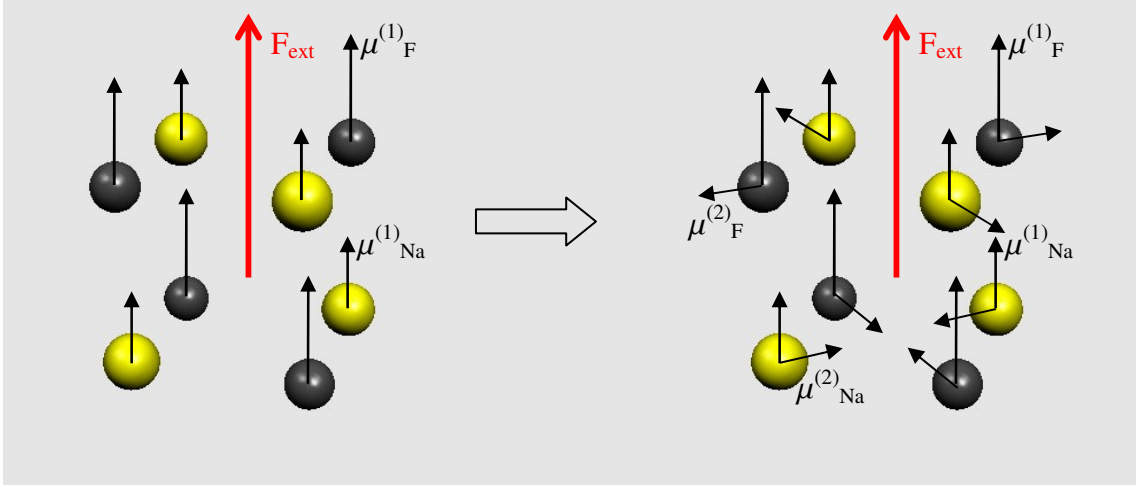
The fields of all first order dipoles then induce the second order dipoles.

$$\mu_{Na}^{(2)} = \alpha_{Na}\left(\frac{3}{4d^3}\mu_{Na}^{(1)} + \frac{\sqrt{2}}{3^{3/2}d^3}\mu_F^{(1)}\right); \quad \mu_F^{(2)} = \alpha_F\left(\frac{3}{4d^3}\mu_F^{(1)} + \frac{\sqrt{2}}{3^{3/2}d^3}\mu_{Na}^{(1)}\right) \quad (3.8)$$

In (3.8) the first contribution in both parentheses comes from dipoles of the same species, the second one from the other species. We checked the error made when stopping at this level compared to the full self-consistent calculation and found it to be less than 5% for these specific ionic polarizabilities, which is acceptable for our purpose. Now (2.65) is used to compute Θ_{xy} and gives the result:

$$\Theta_{xy} = \frac{9}{2^{3/2}}\frac{1}{d^2}(\alpha_{Na} + \alpha_F)(\alpha_{Na} - \alpha_F)F_{ext} \quad (3.9)$$

Since $4(\alpha_{Na}+\alpha_F)$ has to reproduce the electronic DFT polarizability of $6.95*10^{-24}$cm^3 we can use this result and formula (3.9) to get the two ionic polarizabilities. Writing (3.9) with the computed DFT results yields:

$$\Theta_{xy} = 2.75\,a_B(\alpha_{Na} - \alpha_F)F_{ext} \quad (3.10)$$

Using (2.66), (3.10) and $\alpha_{Na}+\alpha_F= 1.74*10^{-24}$cm^3 the following estimate can be made:

$$\alpha_{Na} = 0.65\cdot10^{-24}\,cm^3 ; \quad \alpha_F = 1.09\cdot10^{-24}\,cm^3 \quad (3.11)$$

Keeping in mind that the ions would not be considered as completely ionized, this result is quite reasonable.

3.3 Conclusion

Reviewing this research project it becomes apparent that DFT is a powerful theoretical tool. It can be used for the calculation of a broad range of atomic or molecular properties. However, it would be very welcome if methods were worked out to better estimate the error made in those calculations. The quality and worth of the output would be greatly increased with the computation of error bars. On the one hand there exists the basic error made with the choice of the E_{xc}-functional, on the other hand there are the numerical errors originating from the integration mesh, the self-consistent field convergence criterion and the force convergence criterion of the nuclei. Still, the calculated numbers agree very well with experiment.

In our calculations we found an increased molecular electronic polarizability compared to the free ions. The reason is the residual charge in the Sodium 3s orbital, which has huge dipole transitions to the 3p states. These transitions already explained the large α of the Na atom. Furthermore, we examined the vibrational spectra of a range of clusters, also with respect to their IR-activity. For Na_4F_4 we calculated the properties of two energetically very close structures, the ring and the cube. Most of the results showed fundamental differences. They can be explained with variations in the ionic conformation. Using the energies of larger clusters a guess for the formation energy of the bulk crystal can be made. The result was already very satisfactory and can easily be improved by further calculations. Finally, we could not confirm the symmetry breaking of the $Na_{14}F_{13}$ cluster found by another group.

Concerning classical models, it has to be accepted that they cannot take account of all observed features. One is better advised to mainly use them for visualization and applications to specific cases. Then they are a highly welcome and useful tool and can be used as general guidelines when solving problems.

References:

[1]   P. Hohenberg, W.Kohn; Phys. Rev.; Vol.136, No.3B; p.864; **1964**

[2]   W. Kohn, L. J. Sham; Phys. Rev.; Vol.140, No.4A; p.1133; **1965**

[3]   C. Fiolhais, F. Nogueira, M. Marques; 'A Primer in density funcional theory';
         Springer-Verlag ; **2003**

[4]   M. R. Pederson, K. A. Jackson; Phys. Rev. B; Vol.41; p.7453; **1990**

[5]   K. A. Jackson, M. R. Pederson; Phys. Rev. B; Vol.42; p.3276; **1990**

[6]   M. R. Pederson, K. A. Jackson; Phys. Rev. B; Vol.43; p.7312; **1991**

[7]   A. A. Quong, M. R. Pederson, J. L. Feldman; Solid State Commun.; Vol.87;
         p.535; **1993**

[8]   D. V. Porezag, M. R. Pederson; Phys. Rev. B; Vol.54; p.7830; **1996**

[9]   D. V. Porezag; PhD thesis: http://archiv.tu-chemnitz.de/pub/1997/0025; **1997**

[10]   A. Briley, M. R. Pederson, K. A. Jackson, D. C. Patton, D. V. Porezag;
         Phys. Rev. B; Vol.58; p.1786; **1998**

[11]   M. Hargittai; Chem. Rev.; Vol.100; p.2233; **2000**

[12]   F. A. Cotton; 'Chemical applications of group theory'; WILEY-interscience; **1971**

[13]   NIST Chemistry WebBook

[14]   Y. Iwadate, K. Fukushima; J. Chem. Phys.; Vol.103, No.14; p.6300; **1995**

[15]   C. Ekstrom *et al.*; Phys. Rev. A; Vol.51, No.5; p.3883; **1995**

[16]   J. Lahiri, A. Mukherji; Phys. Rev.; Vol.153; p.386; **1967**

[17]   H. Haken, H. Wolf; ‚Atom und Quantenphysik', 7.Auflage; Springer-Verlag;
         p.321; **2000**

[18]   M. Douay, *et al.*; Chem. Phys. Letters; Vol.148, No.1; p.1; **1988**

[19]   K. Huber, G. Herzberg; 'Molecular spectra and molecular structure IV. Constants
         of diatomic molecules'; Van Nostrand-Reinhold; **1979**

[20] R. Dickey, *et al.*; J. Chem. Phys.; Vol. 98, No.3; p.2182; **1993**

[21] J. Modisette, L. Lou, P. Nordlander; J. Chem. Phys.; Vol.101, No.10; p.8903; **1994**

[22] Ph. Ghosez, J.-P. Michenaud, X. Gonze; Phys. Rev. B; Vol. 58, No.10; p.6224; **1998**

[23] D. Ham; J. Chem. Phys.; Vol.60, No.5; p.1802; **1974**

[24] J. Geiger, H.-C. Pfeiffer; Z. Phys.; Vol.208; p.105; **1968**

[25] P. Flükiger, H.P. Lüthi, S. Portmann, J. Weber; MOLEKEL 4.3; Swiss Center for Scientific Computing; Manno (Switzerland); **2000-2002**

[26] S. Portmann, H. P. Lüthi; MOLEKEL: An Interactive Molecular Graphics Tool; CHIMIA 54 766-770; **2000**

[27] M. Eisenstadt, G. Rothberg, P. Kush; J. Chem. Phys.; Vol.29; p.797; **1958**

[28] J. Hartley, M. Fink; J. Chem. Phys.; Vol.89; p.6058; **1988**

[29] S. Lapshina, G. Girichev, S. Shlykov; Zh. Strukt. Kim.; Vol.30; p.397; **1989**

[30] S. Cyvin, B. Cyvin, A.Snelson; J. Phys. Chem.; Vol.74; p.4338; **1970**

[31] D. Welch *et al.*; J. Phys. Chem.; Vol.64, No.2; p.835; **1975**

[32] F. Calvo; arXiv:cond-mat/0205428 v1; 21 May **2002**

[33] K. Jug *et al.*; J. Phys. Chem. A; Vol.107, No.20; p.4172; **2003**

[34] A. Buckingham, B. Pullman (editor); Chapter 1 in 'Intermolecular interactions: From Diatomics to Biopolymers'; John Wiley & Sons Ltd.; **1978**

[35] C. Kittel; Introduction to Solid State Physics; 7th edition; Wiley Text Books; **1995**

[36] D.Rayane *et al.*; J. Chem. Phys.; Vol.116, No.24; p.10730; **2002**

[37] U. Landman, D. Scharf, J. Jortner; Phys. Rev. Lett.; Vol.54, No.16; p.1860; **1985**

[38] C. Ochsenfeld, R. Ahlrichs; J. Chem. Phys.; Vol.101, No.7; p.5977; **1994**

[39] M. Tosi, F. Fumi; J. Phys. Chem. Solids; Vol.25; p.45; **1964**

[40] D. Welch et al.; J. Phys. Chem.; Vol.68, No.5; p.2159; **1977**

[41]   R. Hudgins et al.; Phys. Rev. Lett.; Vol.78, No.22; p.4213; **1997**

[42]   J. Doye, D. Wales; Phys. Rev. B; Vol.59, No.3; p.2292; **1999**

[43]   J. Doye, D. Wales; J. Chem. Phys.; Vol.111, No.24; p.11070; **1999**

[44]   M.Wilson et al.; J. Chem. Phys.; Vol.104, No.20; p.8068; **1996**

[45]   A. Rowley et al.; J. Chem. Phys.; Vol.108, No.24; p.10209; **1998**

[46]   P. Madden et al.; Chem. Phys. Lett.; Vol.356; p.437; **2002**

[47]   J. Shanker, H. Agrawal; Can. J. Phys.; Vol.58; p.950; **1980**